Experimental Investigation of Gravel-Pack Sizing Performance in Open-Hole Gravel-Pack (OHGP) Applications

by

José Henrique Bitencourt Zimmermann

A thesis submitted in partial fulfillment of the requirements for the degree of

Master of Science

in

Petroleum Engineering

Department of Civil and Environmental Engineering

University of Alberta

ABSTRACT

This thesis presents a setup for open-hole gravel-pack testing and introduces the experimental results to assess Saucier's (1974) gravel sizing design criteria for gravel-pack applications. A Sand Retention Testing (SRT) was modified to simulate the open-hole gravel-pack (OHGP) scenario. Saucier's (1974) materials and operating parameters were first replicated to validate the SRT design. Next, the equipment was used to assess the gravel-pack performance for highly non-uniform and high fines content formation. The gravel-pack performance was assessed in terms of pressure buildup at the formation and gravel interface as well as gravel-pack impairment.

The operational procedure consists of single-phase brine injection with three different flow stages proposed. The flow stages cover low, intermediate, and high flux rates commonly seen for OHGP applications. Furthermore, a consistent gravel and sand preparation method was followed to guarantee uniform samples. The packing procedure for gravel and sand formation was performed independently. Data analysis consisted of monitoring the differential pressure readings across the cell and gravel-pack structure, measurement of fine and sand particles production, and post-mortem analysis on formation sand and gravel-pack samples. The data generated allowed a better understanding of how fines migration, fines accumulation at the formation and gravel interface, and the accumulation of fines and formation particles inside the gravel-pack structure may vary according to the salinity level of brine injected and the flow rate.

The test matrix includes one particle size distribution (PSD), which presents a uniformity coefficient (UC) equals 12 and fines content of 12%. Three salinity levels were considered, as the salinity level plays an important role in fines migration. The coupon screen used for the tests was

a Wire-Wrapped Screen (WWS) as it is the most common type of screen used in gravel-pack applications.

Measurements indicate that the pressure buildup at the formation and gravel interface is highly dependent on flow rate and salinity level. The gravel-pack impairment is mainly caused by fines even though formation sand particles may enter the gravel-pack structure. The gravel-pack impairment is mostly affected by the quantity of fine particles accumulating inside the gravel porous media. These findings lead to a better understanding of the limitations of Saucier (1974) design criteria for gravel-pack sizing.

DEDICATION

This thesis is dedicated to my core family: Ângela Bitencourt Zimmerman, Telmo Zimmermann, João Arthur Bitencourt Zimmermann, and Júlio César Bitencourt Zimmermann. These are the people who I love the most in the entire world. Furthermore, these are the people who have always supported me, regardless of the circumstances.

ACKNOWLEDGMENTS

I sincerely thank my parents and brothers for the constant encouragement of pursuing education and for continually motivating me to always give my best.

I am thankful to my supervisor, Dr. Alireza Nouri, for providing me the opportunity to be part of his research group. I really appreciate his guidance and encouragement to accomplish this research.

I would like to acknowledge RGL reservoir management Inc. for their technical and financial support and the Natural Sciences and Engineering Research Council of Canada (NSERC) for funding this project through their Collaborative Research and Development (CRD) Grants Program.

Moreover, I am thankful to all the members of our research group, who individually have contributed with uncountable feedback on my presentations and, therefore, helped me to improve the final output.

TABLE OF CONTENTS

LIST OF TABLES

LIST OF FIGURES

LIST OF SYMBOLS AND ABREVIATIONS

Symbols

CHGP	Cased-hole gravel-pack
DST	Drill stem test
d10	Formation sand 10-percentile point
d40	Formation sand 40-percentile point
d50	Formation sand 50-percentile point
d70	Formation sand 70-percentile point
d90	Formation sand 90-percentile point
d95	Formation sand 95-percentile point
D10	Gravel 10-percentile point
D40	Gravel 40-percentile point
D50	Gravel 50-percentile point
D70	Gravel 70-percentile point
D90	Gravel 90-percentile point
D95	Gravel 95-percentile point
ΔP	Differential pressure
δCFP	Concentration of fines produced uncertainty
$\delta \Delta P$	Differential pressure uncertainty
δK	Permeability uncertainty
δq	Flow rate uncertainty
δT	Transducer uncertainty
δTM	Turbidity measurement uncertainty
ESS	Expandable-sand-screen
NTU	Nephelometric turbidity unit
OFA	Open Flow Area
OHGP	Open-hole gravel-pack

PPS	Pre-punched screen
PS	Premium screen
PSD	Particle size distribution
SL	Slotted liner
SRT	Sand retention testing
TM	Turbidity measurement
UC	Uniformity coefficient (d40/d90)
WWS	Wire-wrapped screen

Chapter 1 - Introduction

1.1. Background

Sand production is a worldwide concern that may impact the productivity of oil and gas wells. The extension of problems related to sand production range from the accumulation of sand particles in the bottom of the well, which may require workovers depending on the severity of sanding, up to the erosion of downhole valves, flowlines, pumps, and surface facilities (Coberly and Wagner, 1937; Mahmud et al. 2017). Overall, if there is not a controlling measure, the production of sand particles may become costly.

There are different techniques able to remediate and control sand production. The strategy selected depends mainly on the severity of the expected particle production and the project's economic feasibility (Carlson et al. 1992). The mechanical methods are the most common techniques considered for sand control. Among the mechanical methods, the most popular method is the gravel-pack (Penberthy and Cope, 1992). Gravel-pack consists of installing an adequately sized gravel between the wellbore structure and a centralized inner screen pipe. The gravel works as a filter designed to retain the sand particles from the formation while providing a highly porous media for the fluids flowing from the reservoir towards the well. The proper selection of gravel particle size is essential to increase the chances of succeeding in completing a gravel-packed well. There are different design criteria for gravel sizing available in the literature. The most accepted and commonly used design criteria by the oil and gas industry have been proposed by Saucier (1974).

Saucier (1974) gravel sizing design criteria have been developed based on a set of parameters. The parameters selected by Saucier focus on the fluid flow features. Regarding the formation characteristics, Saucier included the median formation grain size as one of the parameters investigated. The extension of the formation characteristics parameters provides the opportunity to assess Saucier's design criteria further. This approach would generate valuable insights for gravel sizing regarding potential limitations for the gravel design criteria. Therefore, to enlarge the understanding of gravel design criteria limitations, challenging formations with high uniformity coefficient (UC) and high fines content are targeted for this investigation. Moreover, the salinity level effect on gravel sizing design criteria is considered once salinity plays an essential role in

fines migration. The addition of the listed parameters above allows a re-evaluation of Saucier's design criteria for gravel-packed wells.

1.2. Problem Statement

Since the 1930s, the gravel-pack design has been investigated to improve the filtering process of sand formation particles during hydrocarbons production. Initially, most of the investigation focused on a geometric basis for the gravel-pack design. Geometric parameters are related to the gravel to formation size ratio, which would prevent excessive sand production while minimizing productivity loss caused by plugging. Eventually, the influence of hydrodynamic parameters, such as flow rate magnitude, flow rate variability, and gas-liquid ratio (GLR), have also been incorporated into the investigations.

Among all the gravel sizing criteria available in the literature, the criteria proposed by Saucier (1974), has been widely accepted and applied by the oil and gas industry. However, it is debatable if Saucier criteria have been properly assessed for highly non-uniform, uniformity coefficient (UC) higher than ten, and high fines content formations, fines content higher than ten percent.

This study investigates the performance of Saucier (1974) gravel sizing criteria for highly non-uniform and high fines content formations. Such formation features lead to higher instability for arch formation at the formation and gravel interface. The wide variability of particle sizes compounding the formation causes higher instability and higher sand production potential. In addition to that, the salinity level of produced water is also investigated once salinity plays an essential role in fines migration. Salinity levels directly correlate to the attachment and detachment rate of fines from the load-bearing formation particles. Consequently, depending on the combination of such parameters influencing fines migration, highly non-uniform and high fines content formations may hold an essential effect on gravel-pack performance. To pursue the assessment of Saucier’s criteria for highly non-uniform and high fines content formations, a Sand Retention Testing (SRT) facility has been slightly modified for gravel-pack investigation, and a testing procedure has been developed and optimized. The facility and procedure designed can assess Saucier’s gravel sizing design criteria for the investigation proposed.

1.3. Research Objectives

This study presents an SRT setup for OHGP evaluations and assesses Saucier's design criteria for highly non-uniform and high fines content formations. The preliminary step taken to achieve these objectives consists of replicating Saucier's operational parameters and materials (1974) to evaluate the SRT equipment for gravel-pack investigation. In addition to the uniformity coefficient and fines content, the salinity level of produced water is considered a gravel sizing parameter as salinity plays an essential role in fines migration.

In this study, the effectiveness of gravel sizing proposed by Saucier (1974) is evaluated by the pressure drop generated at the formation and gravel interface due to the localized fines accumulation. Moreover, gravel sizing efficiency is estimated by the gravel-pack impairment, caused by the accumulation of formation particles inside the gravel structure and the amount of produced sand.

1.4. Research Hypothesis

Reliability on the SRT facility design for gravel-pack investigation should be achieved by satisfactory testing repeatability. Furthermore, the replication of Saucier (1974) materials and operating parameters leads to the expectation of matching the results encompassing the gravel-pack impairment caused by the accumulation of particles inside the gravel structure and the trends for produced particles. Moreover, the pressure drops recordings across the cell, and the gravel-pack device anticipates the concept of fines migration from the top part of the cell towards the bottom part of the cell.

The fines migration from the top part of the cell towards the bottom part should be governed mainly by the drag forces (acting on particle detachment) and the electrostatic forces (acting on particle attachment). Concerning particle detachment, the expectation is that higher flow rates generate higher drag forces, impacting more extensive mobilization of fine particles. Regarding the salinity level, for lower salinity levels, the fine particles tend to deflocculate and, consequently, higher dispersion of fines should occur. The deflocculation of fine particles should induce higher fines mobilization once the particles would be carried through the porous media effortlessly. As the salinity level increases, the fine particles tend to acquire more resilient bonding forces, and consequently, higher drag forces are required to carry these particles through the porous media.

In respect of the gravel-pack performance, a higher quantity of fine particles displaced from formation sand and carried towards gravel-pack structure should decrease the gravel-pack performance (retained permeability) due to the fine particles accumulation expected in the gravel-pack porous media. Consequently, lower salinity and higher flow rates should negatively impact the gravel-pack performance.

The assessment of Saucier's (1974) design criteria for highly non-uniform and high fines content formation should result in a higher gravel-pack impairment. Higher gravel-pack impairment expectations occur since a higher uniformity coefficient leads to higher instability for arch formation at the formation and gravel interface. Moreover, higher fines content should increase the fine particles accumulation inside the gravel-pack structure. Hence, highly non-uniform and high fines content formations with low salinity levels, and submitted to high flow rates, should aggravate gravel-pack impairment.

1.5. Research Steps

This study follows the corresponding steps presented below:

1. Proposal for the design of the SRT facility for open-hole gravel-pack investigation.
2. Evaluation of SRT facility design by performing repeatability tests and replicating Saucier's (1974) operating parameters.
3. Constant optimization of SRT facility and its units during the performance of tests proposed.
4. Assessment of Saucier (1974) gravel sizing design criteria for highly non-uniform and high fines content formations in OHGP applications.
5. Evaluation of salinity level of produced water on Saucier (1974) gravel sizing design criteria.

1.6. Significance of the Work

This study proposes an SRT design for OHGP investigation. Some modifications from the conventional SRT design are implemented to simulate gravel-packed wells.

Furthermore, this research provides relevant knowledge on the assessment of Saucier's (1974) design criteria for gravel sizing, considering highly non-uniform and high fines content formation in OHGP applications. The importance of understanding the limitations of the most widely

accepted and applied gravel sizing converges to better understanding the limitations of such criteria.

Formations with these specific features, highly non-uniform and high fines content, are more challenging for gravel-packing operations. The fact that the formation particles are non-uniform increases the instability of arches formed against the gravel structure. Furthermore, the formation of new arches takes longer for non-uniform formations. The high number of fine particles implies a higher likelihood of porous media plugging by accumulating fines if gravel sizing is not properly designed. Gravel-packing operations can cost a considerable amount of money; therefore, it is essential to establish the limitations of the design criteria for gravel sizing to maximize the chances of successfully performing the gravel-pack completion. Accordingly, the assessment of Saucier's (1974) design criteria allows a reduction of misleading gravel sizing once a higher number of parameters are considered.

Chapter 2 - Literature Review

2.1. Introduction

Millions of dollars are spent yearly to provide sand-free production or a limited amount of sand production among hydrocarbons. Most of the reservoirs facing sand production issues are unconsolidated and relatively young in geological time scale, mainly from Miocene and younger ages. The bonding properties of such formations are generally weaker once sandstone cementation is a secondary geological process. Therefore, older and deeper formations usually present higher cementation levels (Mahmud et al. 2020). Partially consolidated reservoirs containing immature soft clay or silt are commonly prone to sand production depending on the magnitude of the factors affecting particle mobilization in those specific reservoirs. Despite sand production being commonly linked to unconsolidated or partially consolidated sandstones, consolidated formations may also experience sanding (Tronvoll and Fjaer, 1994).

Factors responsible for initiating sand production may vary depending on the reservoir condition and properties. In a general way, the trigger for sand production is rock failure. Rock failure occurs when the magnitude of stress applied to formation is higher than the formation strength limitation (Mahmud et al. 2020). Unconsolidated and partially consolidated reservoirs are more sensitive to fluid flow effects. Consolidated reservoirs, on the other hand, are more impacted by compressive and tensile failure (Tronvoll and Fjaer, 1994). Whenever the flow rate exceeds critical velocity, solid particles are displaced by the drag forces generated by the flowing fluids, leading to potential sand production. An increase in fluid viscosity potentializes the drag force effect, as more viscous fluids generate larger frictional drag forces on the particles composing the formation. As the drawdown pressure increases, the drag forces generated around the wellbore vicinity rise, consequently increasing the displacement of particles towards inside the well. Flow rate fluctuations also play an important role in sand production as fluctuations affect the stability of arches formed by formation particles. Destabilized arches eventually break down, causing temporary sanding until new arches are formed under stabilized conditions. For water-wet reservoirs, water influx reduces capillary pressure, decreasing sand particles' cohesion constituting the formation; consequently, sand particles' displacement becomes more sensitive to flow forces (Carlson et al. 1992, Renpu 2011, Mahmud et al. 2020). Other causes of sanding include the perforation explosion's impact may damage casing perforation as the formation area around the perforation. Additionally, as the reservoir fluid production occurs, natural reservoir depletion

happens. The reservoir depletion leads to pore pressure reduction, and consequently, the stress on the formation sand increases. The increase of stress on the formation may crush particles, damaging the formation and resulting in sand production if effective stress generated exceeds the formation strength (Carlson et al. 1992, Mahmud et al. 2020)

The consequences of sanding present a wide range of possibilities depending on the amount of sand production experienced. In case the flow rate developed during the production of hydrocarbons is not high enough to move most of the solid particles up to the surface, the sand particles may accumulate on the bottom part of the well over time. The accumulation of particles may eventually require a workover for cleaning up purpose, which leads to a loss of productivity due to the well shutdown time plus the workover cost itself. For scenarios where flow rates are high enough to transport the sand particles up to the surface, erosion of surface facilities, flowlines, pumps, and downhole valves may occur as the sand particles' production generates abrasive condition to the equipment the way up to the surface (Mahmoudi, 2017).

Since sand production commonly occurs worldwide and may lead to high operational costs, many techniques have been developed and implemented to remediate and control sand production. The strategy considered to overcome sand production-related issues depends on the severity of the expected production of particles. A low volume of sand particles may be produced without any action required. In case the necessary facilities are available, sand management strategies may be applied. For high severity sand production scenario, conventional sand control methods may be required. The tolerance to the amount of sand produced depends on operational limitations such as equipment’s resistance to erosion, facility capability for handling sand separation and disposal, and availability of necessary equipment to perform sand cleanup operations from bottom hole wellbore (Veeken et al. 1991, Carlson et al. 1992).

Predicting formation sand potential is essential to understanding which production conditions may lead to excessive sanding. A good understanding of the amount of the expected production of sand allows planning on what strategies can be applied to control the volume of particles produced. As a starting point, relating the past performance of similar wells on the same field is an alternative. Furthermore, formation stability may be acquired during a drill stem test (DST) (Deruyck et al. 1992; Carlson et al. 1992). Additional data on formation strength, usually through core extractions, are required to predict sand potential more accurately, but core samples are not always promptly

available. Other techniques, as logging tools, may be considered for such a task. Sonic and density logging tools are used to predict sanding potential through elastic properties of the formation rocks (Tixier et al. 1975; Stein, 1988; Santarelli et al. 1991; Carlson et al. 1992).

2.2. Sand Control Methods

Different completion techniques have been developed to minimize sand production. The completion methods may be categorized into three main groups: flow rate restriction, chemical methods, and mechanical methods.

The selection of the sand control method is a complex task, which depends on several variables. The reservoir properties and field economics are most commonly the two significant categories assessed to select the optimum sand control method among all the options.

Several reservoir properties variables may be considered during the selection of a sand control method. The number of fines, defined as particles smaller than 44 microns, and the uniformity coefficient (UC) of the formation may be considered depending on the fines content and UC range; different techniques may present better performance (Tiffin et al. 1998). The reduction of the productivity index (PI) caused by the injection of resin, which may decrease the formation permeability, or by the addition of a physical barrier such as a screen and gravel-pack (Shahsavari and Khamehchi, 2018). The length of the production zone and the wellbore inclination angle as some methods may present limitations regarding the completion design (Latiff, 2011). The fluid flow rate, viscosity, and water cut are properties that also impact the sand production; therefore, these variables may be included in the assessment for optimum sand control method.

Moreover, sensitivity and uncertainty analysis are commonly applied to evaluate the factors that affect most of the net present value (NPV) of a project (Shahsavari and Khamehchi, 2018). Standard variables analyzed are the project duration, the oil price oscillation for different scenarios, the forecast of the number of workovers for each method considered, and the possible replacement or maintenance for each technique analyzed.

2.2.1. Production Rate Restriction

The simplest method for minimizing sand production is controlling or limiting the production rate. According to Matanovic et al. (2012), the well is allowed to start producing, and gradually rate is increased until the production of sand initiates or the maximum acceptable production rate is

obtained. The maximum production rate is established by restricting the flow rate of the producing fluid below the particles' critical velocity in the pore channel around the wellbore. This process results in producing fine particles at a controlled rate.

For circumstances that the critical velocity is not reached, the forces acting on a sand particle is less than the cohesive forces holding the particle in place. For such scenarios, the formation of natural sand arches occurs, which helps control sand production. In case the production rate surpasses the critical velocity, these arches will collapse and result in sand production. Reducing the velocity helps to minimize sand production while lowering the hydrocarbon production rate. The production decline correlates to limiting the revenues; therefore, it is not a widely applied sand control technique.

2.2.2. Chemical Methods Used for Sand Control

Chemical consolidation aims to increase the formation's compressive strength, acting as a cement between the sand grains while maintaining formation permeability. The chemical consolidation treatment provides bonding properties to the grains (Fig. 2-1).

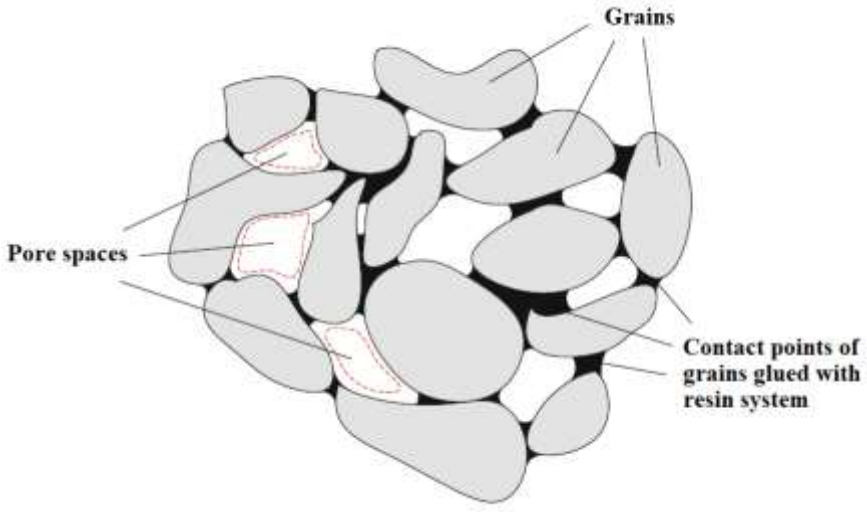

Figure 2-1. Grains contact points after chemical consolidation treatment (Matanovic et al. 2012).

In these methods, chemicals such as plastic resins and polymers are injected into the unconsolidated formations (Mishra and Ojha, 2015). Chemical consolidation is conventionally considered a remedial option and a substitute for mechanical screens for short perforated intervals

with low likelihood and low consequence of sand production (Bellarby, 2009). Two types of chemical consolidation are practiced: (1) in-situ consolidation and (2) resin-coated gravel.

In-situ consolidation involves injecting liquid resins through the perforations into the formation and have those flushed by a catalyst for cementation of the sand grains at their point of contact. The resin, once injected, bond the particles together, creating a permeable stable matrix. The presence of clay minerals may affect the resin performance. If there are clay minerals in the formation, a clay stabilizer should be used before flushing the resin. The amount of resin injected should be balanced to avoid either not enough consolidation strength provided due to the low amount of resin or reduction of permeability caused due to the high resin injection volume (Carlson et al. 1992, Matanovic et al. 2012).

Resin coated gravel involves a coating gravel-pack with a thin layer of highly permeable resin. This gravel-pack is circulated through coiled tubing inside the casing or open-hole. It is then compacted to form a plug across the production path as a permeable filter hardened and strengthened with resin coatings. The main advantage presented by the resin-coated method is that there is no need for special hardware during the installation procedure. On the other hand, the method presents severe additional drawdown generated, affecting well productivity (Carlson et al. 1992).

2.2.3. Mechanical Methods Used for Sand Control

Mechanical sand control methods include two main approaches that can be used individually or in combination: slotted liners and pre-packed screens and gravel-pack. These methods keep the sand in the formation by creating a physical barrier between formation and wellbore while maintaining optimum well productivity, if designed and selected wisely based on three fundamental design parameters: (1) optimum width of slotted liner or screen slot (with and without gravel), (2) optimum gravel size and distribution, and (3) effective placement technique (Matanovic et al. 2012).

The slotted liner and screen approaches are discussed in the following subheading, while the gravel-pack method is presented in the next heading. The presentation of gravel-pack happens in a separate heading since it is further explained in detail.

Slotted Liners (SL) and Pre-Packed Screens

Slotted liners configuration is a low-cost filtering option that provides excellent mechanical strength and structural integrity. According to Xie (2015), the SL design primary objective consists of guaranteeing the structural capacity, providing appropriate sand retention, and a large enough open flow area (OFA). The OFA achievable by SL is limited to the range of 2 to 3% only. There are different slot configurations available for SL (Fig. 2-2). The most conventional slot configuration is the straight cut slot, which presents the same slot size across the entire slot structure. The keystone cut slot and the rolled/seamed top slot present different slot aperture sizes between the top and the bottom slot structure. The aperture size at the top of the slot is smaller than at the bottom for both keystone and rolled/seamed slots. The keystone cut slot was designed to decrease the amount of finer particles produced by the narrower path and further the passage of produced sands through the cut slot structure itself, preventing potential plug inside the slot by the wider path. The rolled/seamed top slot was designed as a modification of the keystone cut slot. When under stress, the rolled/seamed top slot is plastically deformed around 1-millimeter inwards, increasing the top and bottom aperture size ratio and, consequently, varying the production's performance (Guo, 2018).

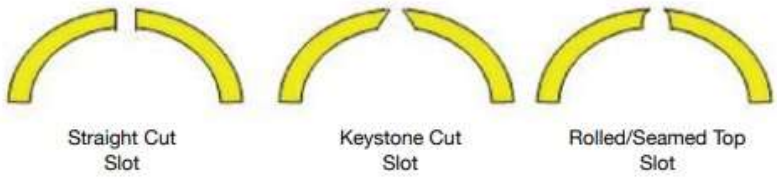

Figure 2-2. Slotted liner slot configuration (Bennion et al. 2009).

There are three different slot patterns available for SL (Fig. 2-3). According to Xie (2007), the overlapping slot pattern regularly presents problems related to overcoming the load stresses applied due to field conditions. It has not been applied as often as standard/staggered and gang patterns.

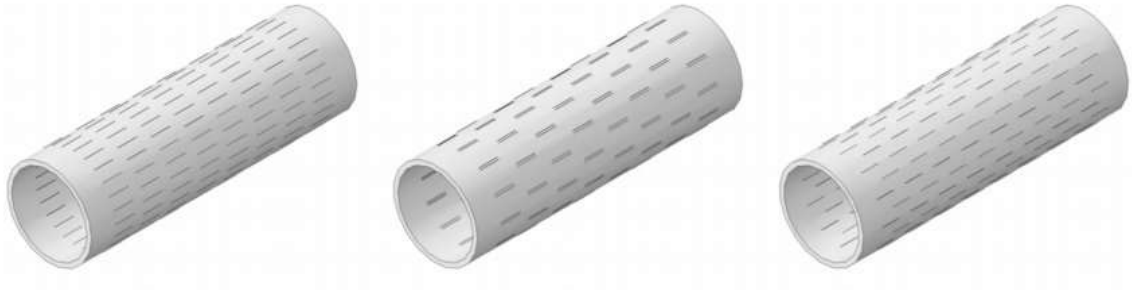

(a) Standard / Staggered (b) Gang (c) Overlapping

Figure 2-3. Slot patterns (Xie, 2015).

The wire-wrapped screen (WWS) was designed by Layne (1918) (U.S. Pat. No US6298914B1). It consists of a wire embracing a perforated pipe to create grooves along with the pipe structure, producing a funnel effect, and, consequently, allowing communication between the external and internal parts of the pipe.

There are different designs for WWS, depending on the application, and the design may vary from one up to more than two wire layers. Usually, WWS is applied either for stand-alone or gravel-pack completions. The WWS is picked for specific field operations considering different features such as aperture size, screen strength, plugging and erosion resistance, laboratory testing, and previous field applications (Matanovic et al. 2012).

The WWS presents a higher OFA when compared to different stand-alone screens, between 5 and 12%, depending on features such as wire thickness and slot width. For gravel-pack applications, WWS is commonly selected over SL due to a few reasons. The WWS design provides some self-cleaning action as the fluid produced gets through the screen. The slot trapezoid shape generates a self-cleaning condition as the flow converges through the available space. Furthermore, the pressure drop generated across WWS is minimized due to the higher OFA. Besides, WWS is more resistant to corrosion once it is manufactured with stainless steel, providing a longer life for the screen, and minimizing severe plugging condition due to corrosion over time (Renpu, 2011).

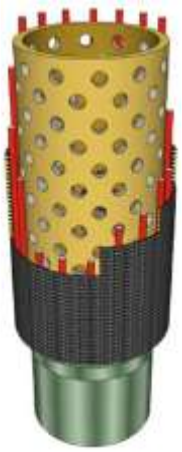

Figure 2-4. Wire-Wrapped Screen design (Matanovic et al. 2012).

In addition to WWS, other mechanical screen methods are available: punch screens, premium screens, and expandable screens. Punch screen consists of a perforated base pipe with a punched shroud for sand filtration. The OFA for punch screen ranges from 1.5 to 8%. Different pre-packed screens are applied in the industry, including double-layered wire-wrapped screens or pre-packed with micro-screens, and single-wire pre-packed screens (Matanovic et al. 2012). Punch screen has been mainly applied in SAGD/CCS horizontal open-hole scenarios.

Figure 2-5. Punch Screen (Variperm Canada Limited).

Expandable-Sand-Screens (ESS) has been designed to eliminate annulus space between the screen and formation wall by expanding the screen structure itself. The fact that the screen physically supports the formation would generate extra well stability once it has been expanded. Moreover, a larger flow area is achieved by superior inner diameter leading to higher well productivity. An ESS structure consists of three layers: base pipe, filter media, and outer protective shroud (Ismail

and Geddes, 2014). Figure 2-6 below illustrates the three layers of ESS for both unexpanded and expanded setups.

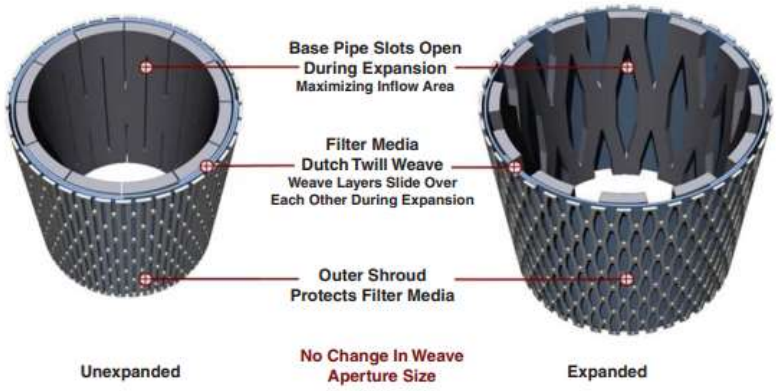

Figure 2-6. Expandable-Sand-Screen (ESS) (Ismail and Geddes, 2014).

2.3. Gravel-Pack

Gravel-pack consists of placing sized gravel in between the wellbore wall and the screen completion. The gravel works as a filter to prevent formation particles from being dislodged by the produced fluids. Gravel-pack has been widely applied in the oil and gas industry for the past decades. Even though the first records of gravel-packed completion for oil wells are from the 30s (Coberly and Wagner, 1937), the method remains prominent nowadays as a means for sand control (Penberthy and Shaughnessy, 1992). Figure 2-7 below presents the two main gravel-pack methods, open-hole gravel-pack (OHGP) and cased-hole gravel-pack (CHGP).

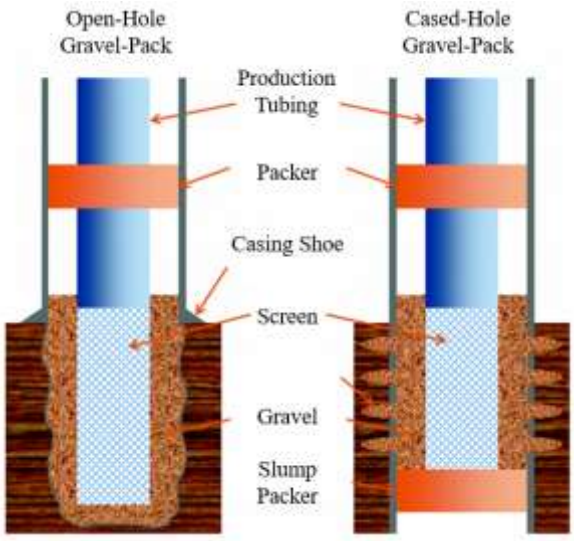

Figure 2-7. OHGP and CHGP comparison (Syltoy, 2014).

For OHGP completions, there is no casing structure between the gravel-pack and the formation sand. Since there is a less physical limitation, naturally, OHGP provides higher productivity when compared to CHGP. The main disadvantages of OHGP completion are the difficulty in isolating water and gas zones. Furthermore, not all the formations can provide wellbore stability for an OHGP completion due to formation strength.

Considering CHGP completions, there is gravel placed in between the perforated casing and the screen completion. The productivity generated by CHGP completion is generally considerably lower than for OHGP, especially if perforations are filled-up by sand formation. In case perforations are properly filled-up by gravel, higher permeability is achieved in the perforation area, and consequently, higher productivity and long-life completion may be feasible. Pre-packing is the term used for when the CHGP is performed with gravel fulfilling the perforations and its surrounding areas. Perforation packed, on the other hand, means that perforations are occupied by formation sand instead, which would drastically impact productivity (Penberthy and Shaughnessy, 1992). An advantage of CHGP configuration is the possibility of isolation of water and gas zones. Moreover, CHGP provides additional wellbore stability since the casing works as a solid structure preventing the formation's collapse.

2.3.1. Formation Sand Sampling for Gravel-Pack Design

The design of gravel-pack pursues the objective of controlling sand production while minimizing productivity loss. The productivity loss may occur due to fines accumulation at the formation and

gravel interface and inside the gravel itself. Fines are defined as particles smaller than 44 μm (as suggested by Abram and Cain, 2014) of loose solid material. The production of fines is beneficial as long as excessive fines accumulation is preventable. To effectively design the gravel to control sand production, and maximize productivity, collecting a representative sample of the formation is essential.

There are different techniques for collecting samples of formations to obtain the particle size distribution (PSD) for the corresponding completion interval. Furthermore, due to the common reservoir's heterogeneity, the PSD often varies across the completion interval.

The most representative sampling method is conventional core samples, commonly taken by rubber sleeve for unconsolidated formations. An adequate manner of proceeding with core sampling is to acquire samples for the complete length of the formation interval (Matanovic et al. 2011). Conventional core samples lead to a high cost and consequently are not commonly available.

As an alternative, sidewall core samples may be considered. Sidewall samples are the most widely used type of sampling for gravel-pack design. Sidewall cores are obtained by a gun placed inside the well at the desired depth for sample extraction. The gun uses projectiles that penetrate the formation and are posteriorly pulled out by an attached line. Even though sidewall samples are considered a decent sampling method, there are some drawbacks to this method. The projectile's penetration impact crushes some of the particles around the formation entrance, plus some drilling mud solids may also be collected among the sample. Both smaller particles generated by the projective impact and the drilling mud solids may lead to a smaller median formation size (Himes and Ruiz Jr., 1986).

Furthermore, core sampling may be performed by bailed samples. Bailed samples are collected from the bottom of the well by wireline. This method is relatively simple to accomplish, but it may lead to unrepresentative samples for the formation. The assumption for the bailed sample method's inaccuracy is that the finest particles are produced to the surface. In contrast, the bigger particles would be deposited on the bottom part of the well first, followed by smaller particles. Therefore, gravel-pack design based on bailed samples may be biased to the larger-size grains increasing the probability of gravel sizing bigger than recommended (Maly and Krueger, 1971).

The least reliable sampling is the produced sample. Produced samples are originated from the particles carried out up to the surface. Besides that, these particles are easily contaminated during production. Smaller median grain size of actual formation is expected since the smaller particles are generally produced. Therefore, gravel-pack design based on produced samples may be biased to the smaller-size grains increasing the probability of gravel sizing smaller than recommended.

2.3.2. Gravel Sizing

As gravel-pack for the oil and gas industry has been utilized since the 30s, several studies have been conducted to increase gravel sizing efficiency. Initially, most of the investigations focused on a geometric basis for the gravel-pack design. However, eventually, other parameters, such as hydrodynamic parameters, have also been incorporated into the investigations. Geometric parameters are related to the gravel to formation size ratio, which would prevent excessive sand production while minimizing productivity loss caused by plugging. Hydrodynamic parameters consider how factors such as flow rate magnitude, flow rate variability, and gas-liquid ratio (GLR) would play a role in gravel-pack performance.

Gravel design efficiency has been first investigated for oil and gas applications by Coberly and Wagner (1937). This pioneering work evaluated the bridging of formation in contact with gravel particles, depending on the formation and gravel size ratio, to optimize the formation particle filtration process. Coberly and Wagner (1937) suggested as gravel design point the 10-percentile of the formation (d10) particle size distribution (PSD) curve. Based on the experimental results obtained, the authors proposed that the 10-percentile of the gravel (D10) should be sized as 10x d10. Coberly and Wagner's (1937) design criteria led to a low gravel-pack efficiency rate for field applications, which consequently induced more conservative criteria for gravel-pack.

Hill (1941) suggested a slightly more conservative design as the gravel and formation size ratio should be 8, considering the d10 of the PSD curve as the design point. As practical results described by Hill (1941), field operations increased efficiency regarding sand control. Pump wear was one of the methods used to evaluate sand production decrease for wells gravel-packed by Hill's design criteria. As pump wear is highly dependent on the amount of produced sand, an increase in pump lifetime was taken as evidence for gravel efficiency in retaining formation particles. Even though some improvement was achieved, according to several individual gravel placement cases, Hill's design criteria (1941) would not be suitable for all the wells.

Posteriorly, distinct design criteria have been proposed considering different design points. Schwartz (1969) proposed varying the design point according to the formation uniformity coefficient (UC). For UC lower than five, D10 should be sized as 6xd10. When UC is higher than five and lower than ten, D40 should be sized as 6xd40. Lastly, for UC higher than ten, D70 should be sized as 6xd70. Schwartz (1969) justified the distinct design points due to the variance in gravel sizing if only one design point is considered for non-uniform formations. Schwartz (1969) pointed out that a gravel-formation size ratio of 6 is considered optimum gravel sizing providing the best results for both sand control and minimization of productivity loss. Furthermore, one should not consider gravel-formation ratios of 4 or less once such a small ratio would most likely lead to plugging and consequent loss of productivity. On the other hand, gravel-formation ratios between 10 and 13 would easily allow formation particles to get inside and through the gravel-pack, causing permeability reduction and sand production.

Following the design point of 50-percentile of the PSD curve, Saucier (1974) has become the most widely accepted criteria by the oil and gas industry up to nowadays. Saucier suggests the design point of 50-percentile once in practice, d50 point is usually more practically available than extreme values. The gravel to formation size ratio proposed by Saucier (1974) is 5-6 times. According to the results presented by Saucier (1974), the gravel size range of 5-6 times would provide an adequate balance of satisfactory sand control and minimum gravel-pack impairment. For this investigation, Saucier removed all particles smaller than 10 microns before conducting the tests. The experiments designed by Saucier (1974) accounted for the gravel-pack performance dependence on median formation grain size, median gravel grain size, the mass flow rate of the fluid, time rate of change of mass flow rate, and gas-liquid ratio (GLR).

Penberthy and Cope (1980) performed an investigation on the design and productivity of gravel-packed wells. The authors used a radial model to investigate both uniform (UC = 1.5) and non-uniform (UC = 3.6) formations. The authors suggest that non-uniform sands tend to reduce the bridging effect due to the range of particle size. Penberthy and Cope used similar sand material adopted by Saucier (1974), Miocene sands from Brazos River. The investigation included single-phase and multi-phase injection. Multi-phase injection resulted in higher gravel-pack impairment and higher sand production levels, especially for larger gravel sizes. The authors pointed out that the multi-phase flow condition generates localized disturbances as phases interface interactions occur through the pore throats, and water-wet fines are then mobilized. Penberthy and Cope's

(1980) findings support the findings presented by Saucier (1974) in terms of design point and gravel to formation size ratio. The authors affirmed that d50 seems to be the optimum point for design point, although one single point cannot represent the full PSD curve. Furthermore, the gravel to formation sizing range of 5-6 times presented the best performance for sand control and minimization of gravel-pack impairment for the test conditions investigated.

Leone et al. (1990) affirmed that, for most cases, the design criteria for gravel sizing proposed by Saucier (1974) and later supported by Penberthy and Cope (1980) present satisfactory results in terms of sand control. However, specific scenarios, such wells designed with both fracture stimulation and gravel-pack, in which gravel sizing could be optimized by using larger gravel grains. Larger gravel would provide higher well productivity by diminishing pressure drop at formation and gravel interface. Furthermore, the authors suggest that the previous work presented in literature has been developed using clean river sands instead of formation sands. Such material substitution could lead to conservative gravel sizing due to the minimum quantity of cementing material present in the washed river sand samples. As the cementing material would bond fine particles together in a real reservoir scenario, the lack of such material leads to a gravel design able to stop the migration of individual particles. According to Leone et al. (1990), this approach would result in a conservative design once the cementing material is present in reservoirs aggregating two or more fine particles as one bigger particle. The agglomeration resulted from specific reservoir conditions changes the critical size parameter for gravel sizing. Leone et al. (1990) used the formation core plugs to overcome this limitation. The results reported by the authors indicate that adequate sand control was achieved for gravel to formation size ratios up to 16:1. The authors concluded that the larger gravel size achieved such performance, mostly due to the mixed-layer clay cementing material present in the samples, which led to particles' agglomerated mobilization.

Oyeneyin et al. (1992) pointed out that the standard design criteria applied for gravel sizing, initially proposed by Saucier (1974), do not consider enough parameters to perform the gravel design efficiently. The authors affirm that even though extensive research has been developed on placement techniques and types of carrier fluids, operators have still reported a high gravel-packed wells failure rate, especially for poorly sorted and unconsolidated formations. The authors attributed the high rate of failure to the general one-point percentile design formulae used for gravel sizing. According to Oyeneyin et al. (1992), a revaluation of the gravel-pack design criteria

should be performed, considering operational conditions previously not considered to provide efficient sand control and reasonable production capacity.

Tiffin et al. (1998) introduced a new design criterion dependent on the formation's fines content and uniformity coefficient. The authors affirmed that for scenarios with a uniform formation and relatively low fines content, the traditional design criteria, introduced by Saucier (1974) and Penberthy and Cope (1980), could be considered conservative due to the excessive restrictive design provided by the 5-6x gravel and formation size ratio. Instead, bigger gravel-sizing should be considered to minimize productivity loss once uniform sands generate higher stability due to the bridging achieved by the narrower sizing range of particles. Furthermore, a combination of a low quantity of fines and high uniformity coefficient would allow a bigger gravel selection, minimizing potential plugging effect caused by fines accumulation. In addition to the uniformity coefficient and fines content, Tiffin et al. (1998) also considered the ratio d10/d95 as a parameter for gravel-sizing. The authors affirmed that the gravel-formation interface is the most critical point for preserving gravel permeability. The fine particles reaching the interface can easily damage the interface permeability if accumulation starts occurring at this point. The d10/d95 ratio is considered a parameter since, for formations in which a high quantity of fines is present, the d10/d95 ratio increases sharply. Tiffin et al. (1998) also compared synthetic and natural gravels, and synthetic gravel presented general improvement for all the tests reported. The authors' suggestion for gravel sizing is the gravel-formation ratio in the range of 7-8x for formations with d10/d95<20, d40/d90<5, and fines content < 5%. The ratio of 7-8x can be adopted in combination with a screen able to handle all the fines for formation within the limits of d10/d95<20, d40/d90<5, and fines content < 10%. For formations with d10/d95>20, d40/d90>5, and fines content > 10%, wellbore enlargement should be considered to increase the distance of gravel and formation interface the wellbore.

Although Tiffin et al. (1998) have reported several tests, the authors have performed only a couple of tests for formations with UC > 10 and fines content higher than 10%. Furthermore, for both tests performed, the gravel was sized as 4x and 1.7x d50, which is considerably smaller than the standard criteria proposed by Saucier (1974). Both gravels failed in terms of performance. The test in which gravel D50 was sized 4x formation d50 presented a considerable amount of production sands. In contrast, the gravel D50 sized 1.7x formation d50 present no sand production, but at a

productivity cost once the high accumulation of fines was reported at the gravel and formation interface. The gravel impairment obtained during both tests described was not provided.

2.3.3. Gravel Quality Assurance

The gravel quality assurance plays an essential role among the different parameters which may impact the gravel-pack performance. There are specifications available in the literature that should be followed to select gravel with minimum-quality for gravel-pack applications.

The gravel quality requirements suggest limits for the percentage of particles exceeding the gravel sizing boundaries and gravel uniformity coefficient (UC). Other quality requirements include the strength of gravel, sphericity, roundness, and mineralogy.

According to Renpu (2011), there are limits for the particle content beyond upper and lower mesh boundaries for the gravel size selected. Gravel particles larger than the upper boundary and smaller than the lower boundary should not exceed 1% and 2% weight percentage in the final gravel PSD, respectively. Concerning the UC, this value should be around 1.5. According to the API standard, the material should provide enough strength to avoid exceeding the weight percentage of crushed material for specific gravel grain size regarding the gravel's strength. The acceptable weight percentage of crushed gravel for gravel size in the range of 16/60 Mesh is 2%. This percentage increases as gravel grain size increases, 12/20 (4%), and 8/16 (8%). Regarding sphericity and roundness, the mean value for both features should be higher than 0.6. About mineralogy, the API standard specifies that gravel mineralogy should be single quartz grain.

2.3.4. Gravel-Pack Evaluation

Once the gravel-pack method has been selected, designed, and properly placed, a couple of factors may be evaluated to measure how satisfactory gravel-pack procedure has been performed. Factors analyzed are possible voids generated during gravel placement and gravel-pack performance assessment through additional differential pressure created by the gravel structure.

Possible voids in the gravel-pack structure would affect the gravel-pack performance. Therefore, there is a necessity of verifying potential locations with poor gravel placement. For such a task, ISOPAC particles may be considered. Individual ISOPAC particles contain isotope surrounded by a resistant shell structure; thus, a gamma spectroscopy tracer log is used to monitor how accurate the gravel particles' placement is conducted. In case voids are found, a wireline shaking tool is

used to create minor turbulences to break down the localized structures preventing the gravel particles from aggregating themselves. These turbulences help gravel particles properly settle down into the voids (Carlson et al. 1992).

Gravel-pack performance assessment may be conducted by performing a drill stem test (DST) before the packing procedure. This approach allows identifying the additional pressure drop caused by the gravel-pack placement. The same performance assessment may be conducted over time as pressure drop increase over time may imply fines moving towards the wellbore and accumulating nearby the formation and gravel-pack interface. Furthermore, for cased-hole completions, the additional pressure drop could also be caused by the collapse of individual perforations (Carlson et al. 1992).

2.4. Fine Particles Migration

The fines' production is beneficial if the fines mobilized can pass through formation pore throats, formation and gravel interface, and the gravel-pack itself. The production of fines prevents the plugging effect and gravel-pack impairment. A significant difference should be pointed out between load-bearing solids and formation fines. The formation fines are loose solid particles, which are not part of the mechanical formation structure. Consequently, these fines end up being carried away effortlessly by drag forces created during flow towards the well (Penberthy and Shaughnessy, 1992).

Formation damage led by pore blockage may occur by the mobilization, migration, and straining of particles in the pore throats (Fig. 2-8) (Russell et al. 2018; Haftani et al. 2019). The same event may be registered for gravel-pack structures if the gravel-pack is designed for a full stoppage of particles. Depending on the formation characteristics and production conditions, severe fines accumulation at the formation and gravel interface and inside the gravel-pack may occur. This phenomenon may generate high productivity loss.

There are physical and chemical interactions between fluids and particles in the reservoir, which affect the migration of fine particles (Gabriel and Inamdar, 1983). Both physical and chemical interactions play an essential role in fines migration. There are some primary and secondary forces acting on individual particles: lifting force, *Fl*, hydrodynamic drag force, *Fd*, electrostatic force, *Fe*, and gravitational force, *Fg* (Fig. 2-8) (Russel et al. 2017).

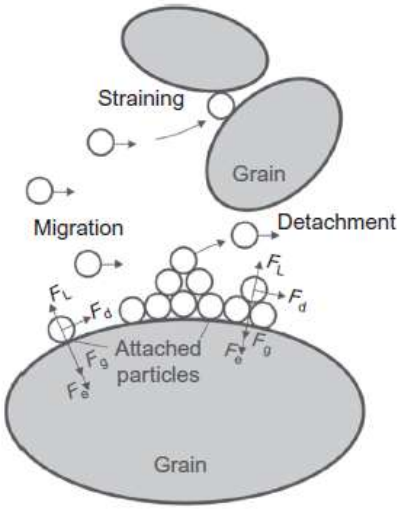

Figure 2-8. Primary and secondary forces acting on individual particles (Russel et al. 2018).

According to Russel et al. (2017), hydrodynamic drag forces and electrostatic forces play the most critical roles in the attachment and detachment concentration of particles during flow conditions. Lifting and gravitational forces are secondary forces acting on the particles. Aji (2014), points out that when formation fines are attached to load-bearing particles, hydrodynamic and electrostatic forces balance alteration can modify initial condition during flow towards the well. The equilibrium between particles may be disturbed depending on the dominant forces acting on these particles, leading to either detachment of formation fines or an increase in attachment conditions. In case the hydrodynamic drag forces generated are higher than the electrostatic forces holding the particles together, the formation fines are carried away. When such a condition is achieved, the flow velocity is beyond critical velocity for fines movement under specific reservoir conditions.

2.4.1. Hydrodynamic Drag Forces

The hydrodynamic drag forces induce the detachment of fines from the grain surfaces. The carrier fluid velocity, fluid viscosity, and particle size are the most critical variables dictating how intense hydrodynamic forces are. Higher carrier fluid velocity and viscosity increase the probability of fines to detach from the formation grains. Furthermore, a larger particle cross-sectional area also increases the hydrodynamic forces; therefore, larger fines diameter increments the likelihood of fines mobilization throughout the porous media.

Since hydrodynamic drag forces are highly dependent on fluid flow velocity, as higher fluid flow velocities are developed in the porous media, it increases the mobility of fines. When a sudden

flow injection, high enough to mobilize fines, occurs in the porous media, an instant increase in the porous media permeability is seen due to the localized displacement of fines (Khilar and Fogler, 1998; Sarkar and Sharma, 1990; Russel et al. 1998). The larger quantity of fines displaced leads to the possible increment of fine particles' straining within the formation grains. The rise in the straining of fines happens due to the larger number of fines mobilized at the same time and moving through a limited physical space, which is the porous media. Consequently, fine particles' retention concentration starts building up as more fines accumulate in the restrictive porous. The retention concentration eventually reaches a maximum level, which can no longer rise. The limitation of retention concentration of fines happens because the interstitial velocity generated by the limited interconnected porous is increased to the point that the hydrodynamic forces are high enough to prevent more attachment of fines in the corresponding environment (Russel et al. 2018).

2.4.2. Electrostatic Forces

The electrostatic forces, known as Coulomb forces, are either the attractive or repulsive forces between two electrically charged objects. Salinity levels may increase or decrease these attraction forces between fine particles and pore surface areas (Kia et al. 1987; Mohan and Fogler, 1997; Russel et al. 2017). The total electrostatic force's potential energy source is accounted for mainly by Van der Waals forces and electric double layer (EDL) (Derjaguin and Landau, 1941; Ruckenstein and Prieve, 1976; Gregory, 1981; Elimelech et al. 1995; Russel et al. 2017).

Van der Waals forces are defined as the attraction of intermolecular forces among molecules. This attraction occurs by interaction in the fluctuating polarizations of surrounding particles. This molecular interaction is distance-dependent as the interaction forces disappear for longer distances. Although Van der Waals forces play a role in fines migration, several authors have suggested that electric double layer force acts as the dominant parameter for attachment and detachment of fine particles (Khilar and Fogler, 1984; Sokolov and Tchistiakov, 1999; Russel et al. 2017 and 2018).

Electric double-layer (EDL) consists of two layers on the surface of a particle that has been exposed to a fluid. The first layer, the stern layer, is composed of ions chemically absorbed by the particle surface area. The second layer, the double-layer, is formed by ions attracted to the first layer (Coulomb forces). The second layer is also named the diffusive layer once it is not fixed to the first layer. The second layer interaction with the first layer depends on the electric attraction

and thermal motion of ions freely present in the solution. Figure 2-9 below represents the electrical double layer boundary schematics.

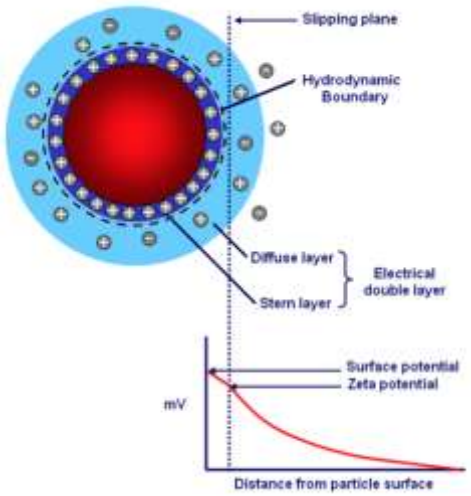

Figure 2-9. Electrical double layer boundary schematics (Russel et al. 2017).

The electrical potential difference between the first and second layers is known as zeta potential. Figure 2-10 below displays the zeta potential (mV) for kaolinite and silica sand according to the NaCl salt concentration (mol/L) (Russel et al. 2017). Both silica sand and kaolinite present the highest negative values for zeta potential at low point NaCl concentrations.

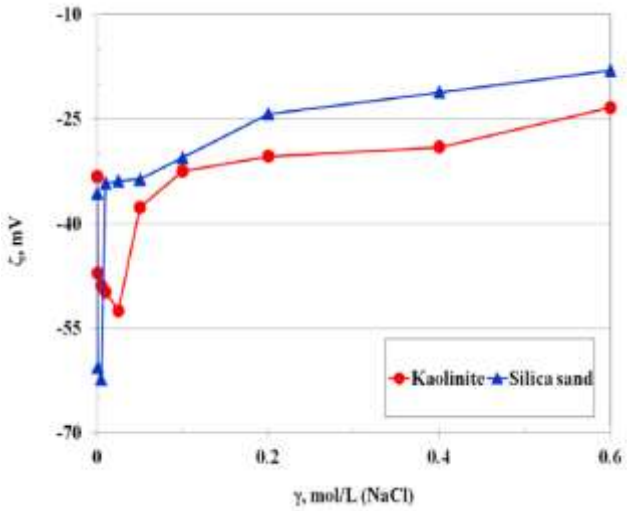

Figure 2-10. Zeta potential for kaolinite and silica sand (Russel et al. 2017)

Sokolov and Tchistiakov (1999) introduced an indicator of fines dispersion potential. This indicator provides a scale of flocculation and dispersion zones. The flocculation and dispersion

zones vary according to the zeta potential magnitude. Zeta potential of particles differs after the salt type and concentration, which impacts the intensity of aggregation or dispersion of particles (Russel et al. 2017; Haftani et al. 2019). Figure 2-11 illustrates the zeta potential scale (mV). The flocculation zone occurs for zeta potentials between -30 and +30. Flocculation occurs considerably faster for the range of -10 to +10. The dispersion zone is registered on both sides of the flocculation zone. Moderate dispersion ranges from -30 to -40 or from +30 to +40. The good dispersion process ranges from -40 to -60 or from +40 to +60. Any range going beyond -60 or +60 is considered excellent as dispersion reaches the highest values. Therefore, low-salinity water is favorable for fines detachment and mobilization (You et al. 2014).

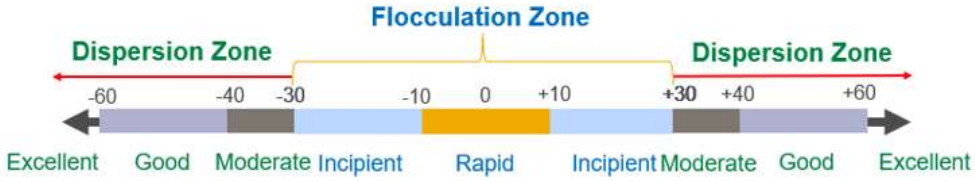

Figure 2-11. Zeta potential scale for flocculation and dispersion zones (Haftani et al. 2019).

2.4.3. Critical Salt Concentration (CSC) on Fines Detachment

There is a critical salt concentration, which has been reported in the literature, for clay particles (Khilar and Fogler, 1983; Khilar and Fogler, 1984). According to these pioneer studies, performed on Barea sandstone cores, once the salinity level of injected brine reaches values below CSC, the sandstone permeability is drastically reduced due to the detachment of fine particles grain surfaces. The immediate high detachment rate of fines provokes fine particles' accumulation in the porous throats, plugging the porous media. The CSC phenomenon does not occur for cations with a valence greater than one and, therefore, it only happens for monovalent cations.

Khilar and Fogler (1983) investigated NaCl as a salt type and kaolinite and illite as the dispersible clays. The sandstone permeability core used by Khilar and Fogler (1983) presented a sharp decrease in its permeability for the range of 4,250-4,000 ppm of NaCl. For values higher than 4,250 ppm of NaCl, there was virtually non-existent formation damage caused by fine particles release.

Chapter 3 - Facility Set-Up and Experiment Design

3.1. Introduction

The facility set-up and the experiment design are critical to replicate the phenomenon occurring under field conditions to its highest possible extension considering lab limitations. Therefore, facility set-up and experiment design are developed to provide a reliable simulation of gravel-packed wells.

The facility set-up and the experiment design have been appropriately developed to provide decent experimental consistency and accuracy. This chapter describes the main facility set-up components and the relevant experiment design points for this research. This chapter presents the testing material used, sand formation and gravel packing preparation, and fluid preparation. Furthermore, the chapter contains the sand-pack and gravel-pack saturation process, flow rates and flow stages design, post-mortem analysis, and experiment design optimization.

3.2. Facility Set-Up for OHGP Investigation

A large-scale SRT facility is used to simulate the near-wellbore region in an OHGP condition (Fig. 3-1). This facility consists of six units: (1) test cell and the main body, (2) fluid injection, (3) data acquisition and monitoring system, (4) back-pressure unit, (5) sand and fines measurement unit, and (6) axial load frame.

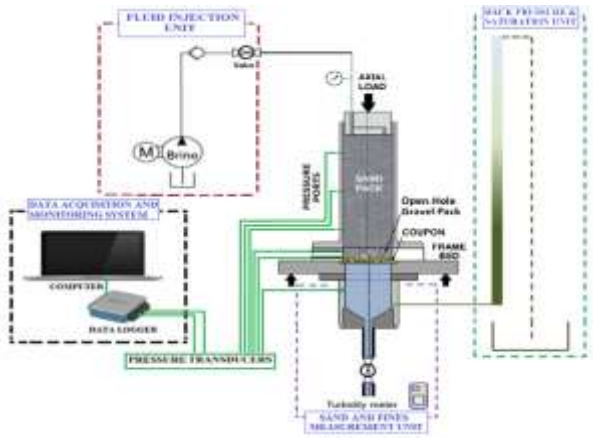

Figure 3-1. Sand Retention Testing (SRT) facility for OHGP investigation.

3.2.1. Test Cell and Main Body

An aluminum cell and an acrylic device make up the test cell. The aluminum cell accommodates the sand-pack, and the acrylic device receives the gravel-pack structure. The aluminum cell's

height and inner diameters are 18.5 inches (47 cm) and 6.03 inches (15.2 cm), respectively. The gravel-pack device's height and inner diameters are 2 inches (5.08 cm) and 6.03 inches (15.2 cm), respectively.

A screen coupon is placed at the bottom part of the gravel-pack device, simulating an OHGP structure with a wire wrapped screen (WWS) completion. Figure 3-2 shows the sand-pack cell, the gravel-pack device, and the WWS coupon placed over the frame bed, making up the SRT facility's test cell and main body structure.

Figure 3-2. Test cell and main body structure.

3.2.2. Fluid Injection Unit

The fluid injection unit comprises two LEWA triplex process diaphragm pumps, which can each deliver up to 60 liters per hour of brine. Both pumps are capable of injecting brine to the SRT cell at different flow rates. According to the desired flow rate, the flow rates are adjusted by fixing certain stroke length and modifying pump frequency through a variable frequency drive (VFD). Flow rates are continuously monitored during the test by a mass balance reading to control fluid injection precisely. Each pump holds a 25-liter tank for brine supply during the test.

3.2.3. Data Acquisition and Monitoring System

The data and monitoring unit includes four differential pressure transducers, with 0.25% accuracy of the full range, and a data acquisition system. The data is acquired by the pressure ports installed across the sand-pack cell and the gravel-pack device (Fig. 3-3). The three differential transducers installed in the sand-pack cell present a pressure range of 50 psi, while the pressure range of the differential pressure transducer used for the gravel-pack device is 2 psi. The data acquisition system includes a data logger, a computer for data recording and display.

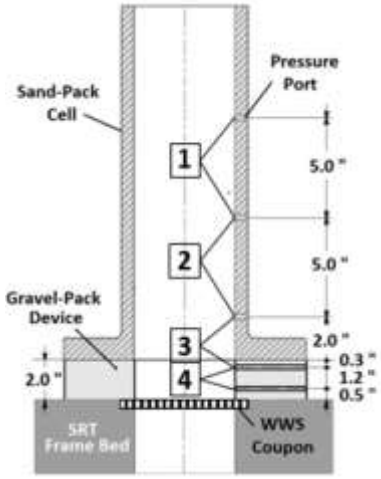

Figure 3-3. Pressure ports locations and distances.

3.2.4. Back-Pressure Unit

The back-pressure column unit provides a minor back-pressure on the sand and gravel-pack during the saturation and flow test phases. This column also makes the required route for effluent. The back-pressure column unit is 185-centimeter long with a 5-centimeter diameter.

3.2.5. Sand and Fines Measurement Unit

Sand and fines measurement unit consists of a sand trap and a fines collection tap. The sand trap is installed at the outlet, capturing the produced sand particles passing through the gravel-pack and WWS coupon. The sand trap can be isolated on-demand to collect and measure the produced sand. A narrow pipe is attached to the sand trap for collecting the outflow samples at any moment. A laser particle size analyzer is employed to plot the PSD of the produced fines in the outflow samples. The quantity of the produced fines (particle smaller than 44 μm) is measured using a turbidimeter device.

3.2.6. Axial Load Frame

The axial load frame comprises a hydraulic piston that may provide up to 500 psi axial stress on the sand-pack. The top platen, which is located over the sand-pack, transfers the load from the load frame to the sand-pack and hydraulically seals the cell using O-rings.

3.3. Experiment Design

The experiment design was arranged in two different sections. The first section corresponds to the replication of Saucier's (1974) operational parameters. An assessment and replication of such parameters have been performed to extend the details available in the literature. For the operational parameters not specified by Saucier (1974), Penberthy and Cope's (1980) research was considered. This decision is supported by the fact that Penberthy and Cope (1980) obtained similar results in gravel-pack design compared to Saucier's findings.

The second section regards the experiment design of highly non-uniform and high fines content formation combined with operational parameters replicating OHGP scenario. The experiment design was dynamically optimized according to the output obtained during initial tests. The outcome of each test used for experiment design optimization is discussed throughout this chapter.

3.3.1. Testing Material and Procedure for the Replication of Saucier (1974) Operational Parameters

Saucier (1974) used a PSD from the recent Miocene sands of the Brazos River. However, Saucier (1974) did not provide further details on the PSD, such as graphical information. Penberthy and Cope (1980), who used the same recent Miocene sands of the Brazos River, made available the graphical PSD, followed for this research. Commercial sands and silts were mixed to replicate the target PSD and match the fines content. Table 3-1 presents the recipe used for PSD replication.

Table 3-1. Commercial sands recipe used for formation PSD replication used by Saucier (1974).

Sil 325	LM125	LM-70
20%	75%	5%

Figure 3-4 below shows both PSDs for Penberthy and Cope (1980) and its replication by commercial sands. There is a good match for most of the PSD, except for the fines content. Both Saucier (1974) and Penberthy and Cope (1980) performed their corresponding experiments without any particle smaller than 10 microns. An attempt to wash out particles smaller than 10 microns by a 10 microns nylon mesh filter was unsuccessful. At the end of the filtering process, around 60 wt% of the particles smaller than 10 microns were still present in the sample. Furthermore, the drying process of the remaining particles is exceptionally time-consuming. The d50 of the sand is 94 microns, and the fines content, particles smaller than 44 microns (as suggested by Abram and Cain, 2014), is 15%.

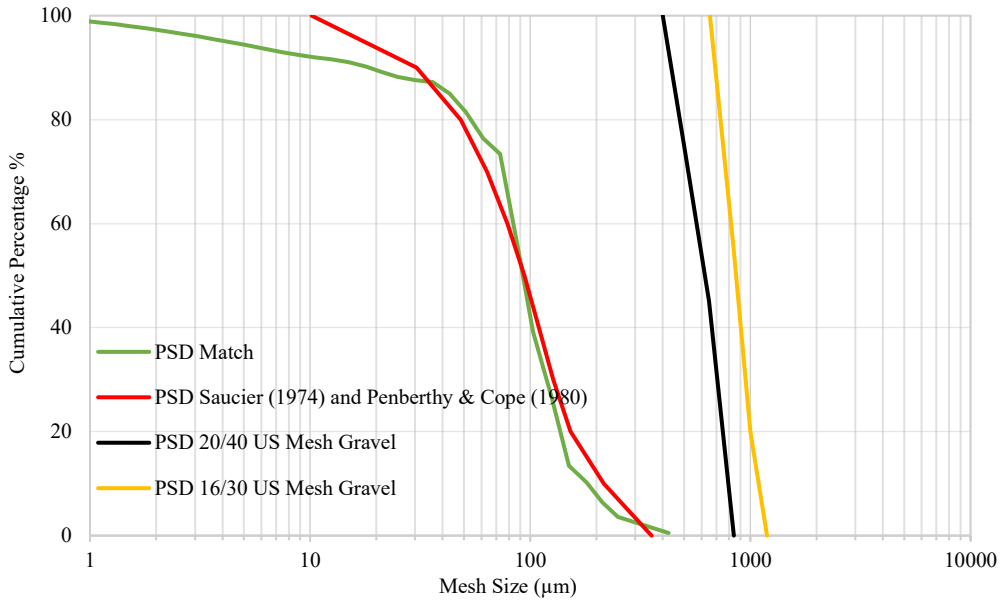

Figure 3-4. Saucier (1974) PSD replication.

The D50 for the two sets of gravel sizes used by Saucier (1974) is 6.7 and 9.4 times bigger than the d50 of the sand (Fig. 3.4). The gravel sizes selected are 20/40 U.S. mesh and 16/30 U.S. mesh. Gravel 20/40 D50 is 630 microns, while gravel 16/30 D50 is 883 microns. The gravel material selected follows quality practices available in the literature regarding uniformity coefficient (UC), sphericity, roundness, and the percentage of particles tolerated beyond boundaries. The gravel quality practices have been previously presented in the gravel quality assurance section. Both sets of gravel sizes 20/40 and 16/30 follow the quality assurance parameters mentioned.

3.3.2. Testing Material and Procedure for OHGP Investigation

Figure 3-5 presents PSD 1, which is the PSD selected to investigate highly non-uniform and high fines content. The UC of PSD 1 is 12, and its fines content is 12%. The match for PSD 1 is also presented in Figure 17 as well as the gravel PSD. Table 3-2 below displays the recipe used for the PSD 1 match.

Table 3-2. Commercial sands recipe used for formation PSD 1 match.

Silt7	Silt1	Kaolinite	LM125
18%	60%	12%	10%

The d50 is 250 microns, while D50 is 1410 microns, which results in a 5.64 times gravel to formation ratio, therefore within the range presented by Saucier (1974) sizing criteria. The gravel range used is 12/16 US mesh (Fig. 3-5).

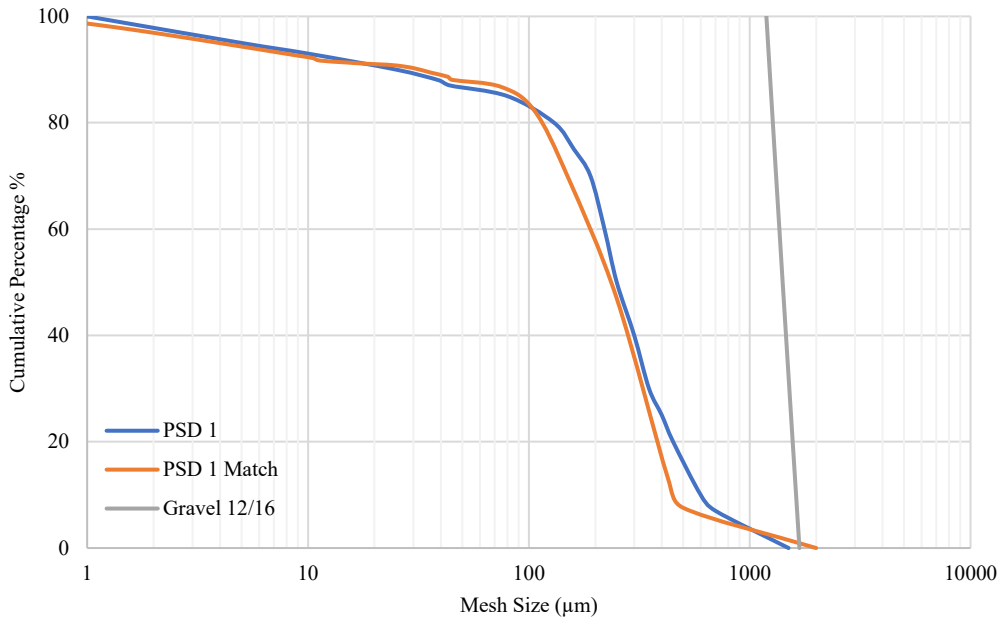

Figure 3-5. PSD 1 match and PSD for the 12/16 US Mesh gravel size.

3.3.3. Coupon and Cell Preparation

Cell preparation is performed by placing wire mesh in the transducer ports to prevent particles from plugging the flow lines connecting SRT cell and differential pressure transducers. Wire-

wrapped screen (WWS) is selected as the screen type for this investigation. Screen aperture size should be wide enough to avoid plugging by fines migrating through the gravel and sufficiently narrow to prevent any gravel particle from being produced. The screen aperture size should be in the range of 50% to 75% of the smallest gravel particle size (Penberthy and Shaughnessy 1992, Bellarby 2009, Roostaei et al. 2018).

3.3.4. Gravel-Pack and Sand-Pack Packing

In the current study, the moist tamping method (Ladd, 1978) was used to packing the sand inside the cell. The procedure is performed in a layer-by-layer step, where the same amount of mass is used for each layer. This method provides consistency in packing regarding porosity and permeability across the cell. A total of 12 kilograms with 10% water content is used, generating 12 layers of formation sand. During the packing, the objective was to reach a minimum porosity by mechanical tamping, to replicate Saucier's packing procedure (1974).

The porosity of 40% is suggested for the gravel packing as field-scale laboratory tests have indicated that low viscosity fluids usually pack in the range of 39-40% (Penberthy and Shaughnessy 1992). Therefore, the necessary mass of gravel to reach the target porosity was estimated considering the gravel samples' specific gravity and the total volume of the gravel-pack device.

The sand was not packed over the gravel to avoid overpacking and disturbance of the gravel. Consequently, the sand was packed separately in the testing cell. Posteriorly, packed sand was placed on top of the gravel-pack device filled by gravel.

3.3.5. Fluid Preparation and Gravel-Pack and Sand-Pack Saturation

The tests are performed with single-phase brine injection. Deionized water is used as the fluid, which receives the addition of NaCl for brine composition. The corresponding amount of NaCl is added to the deionized water to obtain the desired salinity level. The pH of 7.9 was used for all the tests. Before the test, pH is measured and adjusted to reach the desired level of 7.9. Sodium bicarbonate (Na_2CO_3) is used for increasing the pH, while sodium bisulfate ($NaHSO_4$) is added to the brine to reduce the pH level.

The saturation procedure is performed by injecting brine from the bottom of the cell toward the top. A flow rate of 500 cc/hr is used for saturation. This flow rate is low enough to avoid disturbing the sand and gravel-pack.

3.3.6. Flow Rates and Flow Stages for the Replication of Saucier (1974) Operational Parameters

Saucier (1974) performed experiments for cased-hole gravel-pack scenarios, in which the injection of fluid occurred through one single perforation of 0.5 in diameter. Three different flow stages and two different flow rates were considered for each experiment. The first flow stage consisted of injecting 8.7 barrels per day (bbl/day), while for the second flow stage, the injection was 13.5 bbl/day. The injection for the third flow stage was 8.7 bbl/day.

The flow rates used for this research replicate Saucier's operating parameters by assessing the liquid flux and scaling it up to the coupon area used in the OHGP-SRT facility. To properly scale up Saucier's flow rates, the wellbore configuration accounted for should be available. Then, the liquid flux could be assessed, and consequently, the equivalent flow rate for the coupon area in the SRT facility could be estimated. However, since Saucier does not provide the well completion configuration considered, a set of different well completion scenarios was considered to assess Saucier's experiments' liquid flux.

The wellbore completion configuration possibilities include perforation densities, perforation phase angle and wellbore diameters for gravel-packed wells. The perforation densities of 4, 6, 8, 10 and 12 perforations per foot and perforation phase angle of 90°, 120°, and 180° were considered. Moreover, wellbore diameters of 7, 7-5/8, and 8-5/8 inches were used for the calculations. The perforation densities and phase as well as the wellbore diameters were selected because these are typical values for gravel-pack applications in the field.

Figure 3-6 displays the example of assessing the drainage area for 8 perforations per foot and 90° phase angle wellbore. The area in blue color (A1) is known for a certain wellbore diameter. The area in yellow color (A2) can be estimated as one-quarter of A1. Therefore, A2 is the drainage area for one single perforation for the wellbore with 8 perforations per foot and 90° phase angle. From this drainage area (A2), Saucier's liquid flux for the two flow rates is estimated. The same procedure was implemented for all the possible wellbore completion configurations for the corresponding perforations per foot, phase angle, and wellbore diameters.

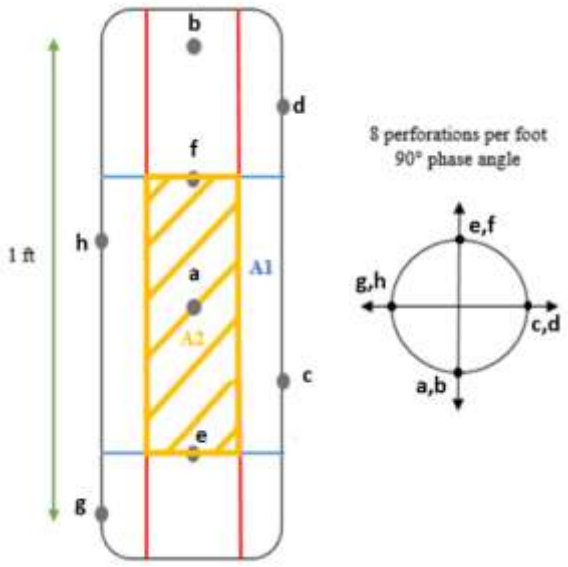

Figure 3-6. Drainage area for flow rate calculation.

Once all the calculations are performed, one single configuration should be chosen as the optimum one. Renpu (2011) stated that an optimum perforation configuration, considering perforation density and phase angle, would result in a minimum interaction between perforations. The minimum interaction between perforations leads to perforation stability for the wellbore. Perforations are more susceptible to failure for high-proximity perforation design, and chain reaction may occur from one initial failure, consequently impacting wellbore productivity.

A reasonable configuration among all the possibilities listed above is 8 perforations per foot, 90° phase angle, and 7-5/8 in diameter wellbore. This configuration provides least interaction between the perforations and therefore, the highest perforation stability among the options considered. Therefore, the flux rates are estimated for the corresponding configuration, considering both flow rates of 8.7 and 13.5 bbl/day. Once flux rates are estimated, the flow rates are obtained by multiplying the flux rates to the SRT facility's coupon area. The flow rates obtained from 8.7 and 13.5 bbl/day are 39,500 cc/hr and 61,500 cc/hr, correspondently.

There are three flow stages; in which the first flow stage lasts 20 minutes from the start point with a flow rate of 39,500 cc/hr. The second flow stage starts at minute 20 by increasing the flow rate to 61,500 cc/hr, kept constant until minute 45. From minute 45 up to 55, the third flow stage is performed at a reduced flow rate back to the initial flow rate of 39,500 cc/hr. The total experiment duration is 55 minutes. Both flow stages and the duration time match the procedure, followed by

Saucier (1974). Figure 3-7 illustrates the flow rates and flow stages adopted. Rapid rum-ups were performed between the flow stages, following Saucier's (1974) rump-up procedure.

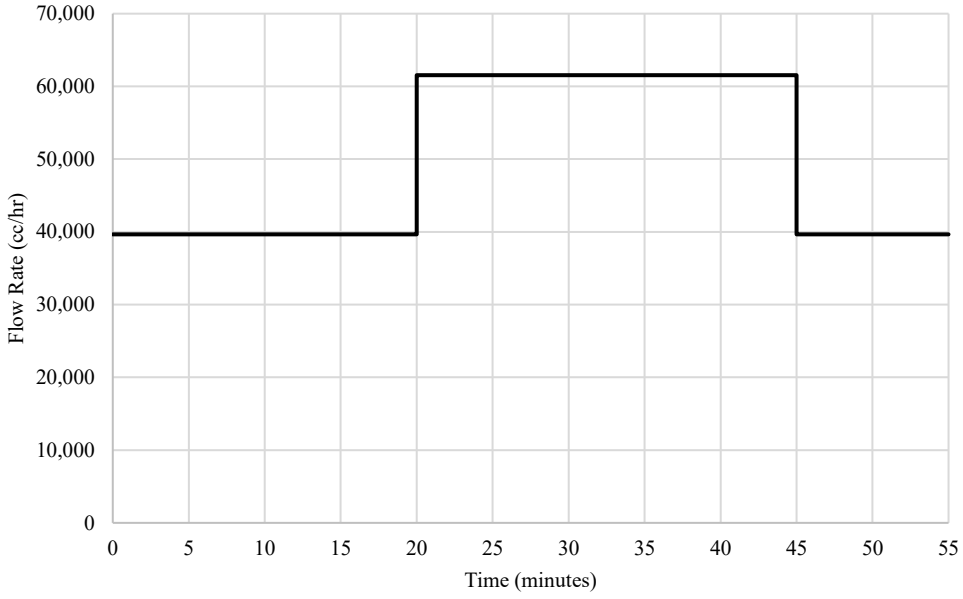

Figure 3-7. Flow rates and flow steps scaled to SRT facility.

3.3.7. Flow Rates and Flow Stages for OHGP Investigation

The flow rates and flow stages for OHGP investigation follow an approach of assessing realistic flow rates for OHGP scenarios and considering three different flow stages. These flow rates analyzed were distinguished as low, intermediate, and high flow rates.

The OHGP wells assessment was performed considering a data set of different gravel-packed wells where flux rates were calculated for a variably of field cases. Once flux rates were calculated, three flux rates were selected as extreme bounds and intermediate flux rates for OHGP applications. These flux rates were scaled to the WWS coupon area used in the SRT facility. Figure 3-8 displays the three flux rates, and the corresponding three flow rates, used for OHGP investigation.

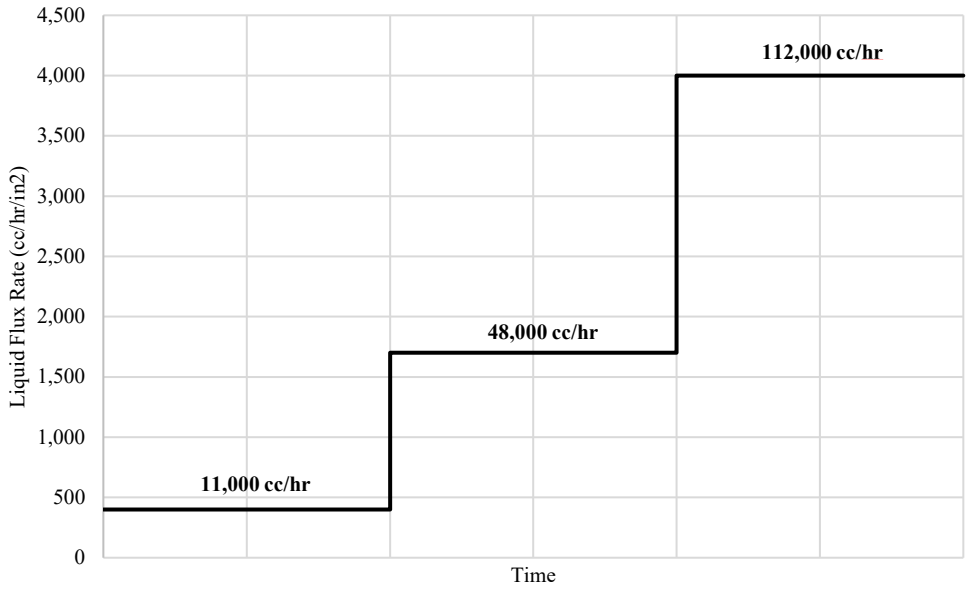

Figure 3-8. Flow rates and flow steps used for OHGP investigation.

The flow stages for the OHGP tests are not constrained by time. Instead, each flow stage is performed until steady-state for both the pressures drop across the sand formation and gravel-pack structure and fines production reach complete stabilization.

The Reynolds numbers for all the tests were estimated to ensure laminar flow during brine injection (Equation 3.1). As turbulent flow or non-Darcy flow commonly occurs for Re > 10 (Rhodes, 1989), the tests performed during this research present exclusively laminar flow condition.

$$Re = \frac{\rho * Dp * v}{\mu} \tag{3.1}$$

where ρ is the density of the fluid, Dp is representative particle diameter, v is the superficial velocity, and μ is the fluid viscosity.

3.3.8. Post-Mortem Analysis

During the flow stages, fluid samples were collected from both the sand trap and fines measurement unit every 5 minutes. The samples obtained from the sand trap passed through a wet sieving technique in which a 44 microns sieve is used to quantify the number of formation particles larger than fine particle size has been produced. Regarding the measurement of fines, a turbidity measurement unit was employed to assess the concentration of fines produced during each step.

After each test, core samples were extracted from the sand-pack formation and gravel-pack structure. A cylinder long enough to penetrate both sand-pack and gravel-pack structures simultaneously was used to bring out the samples. Figure 15 shows the location of each sample taken. A total of 4 samples were taken from each test. The gravel-pack sample was further split into two different samples, top and bottom gravel-pack. Samples were dried in an oven at 120 Celsius degree. Once samples were completely dried out, each sample went through a wet sieving technique using a 44 microns sieve to discard the fines. Once again, the samples were taken to the oven at 120 Celsius to finalize the drying process. By the end of this process, the mass difference measured leads to the number of fines present in each sample analyzed.

3.4. Experiment Design Optimization

A total of three tests were performed for the replication of Saucier (1974) operating parameters. Tests 1, 2, and 3 were successfully operated and generated useful insights that enabled the experiment design's optimization.

By analyzing the results obtained by Tests 1, 2, and 3, oscillations in the differential pressure readings were recorded, although the flow rate measurements indicated constant flow rates. The oscillations occurred to be more significant at the top part of the cell. The reason for such oscillations was the injection system, which was not providing steady flow injection. Therefore, the flow rates were constant, but the injection itself was disrupted.

The injection oscillation problem was tackled by adopting a lower stroke length, and a higher frequency for injection was adopted. On top of that, dampeners were added to the injection flow lines to provide higher flow injection stability (Fig. 3-9).

Figure 3-9. Dampeners added to the injection system.

The tests following Test 3 were performed after the injection system optimization. Therefore, there was no injection oscillation for the test matrix tests presented in Chapter 5 (Tests 4, 5, 6, and 7).

3.5. Uncertainty Measurement

The measurement of uncertainty for the experiments performed was calculated, considering the uncertainty from multiple variables. The variables accounted for are the uncertainties due to measurement limitations. All instruments present finite precision that limits the capacity of measurement. An assessment of the finite precision of these instruments allows for a proper uncertainty measurement.

Electronic transducers measure the differential pressure across the sand-pack cell and the gravel-pack device (ΔP). These electronic transducers have an accuracy of 0.025%. The pressure range of the transducer installed in the gravel-pack ports was 2 psi, while the pressure range of the three transducers installed across the sand-pack cell was 50 psi. Therefore, the accuracy of the transducers (δT) was ±0.005 and ±0.125 psi, respectively. The uncertainty of the differential pressure readings (δΔP) is expressed by Equation 3.2 as:

$$\delta\Delta P = \Delta P * \delta T \tag{3.2}$$

Permeability calculations are a function of the flow rate and pressure drop ratio. Therefore, the error propagation for permeability measurement is calculated by the division error propagation method. Equation 3.3 calculates the uncertainty for the permeability (δK) by considering the

uncertainties of differential pressure (δΔP) and flow rate (δq) as well as the absolute values of pressure drop (ΔP) and flow rate (q).

$$\delta K = |K| * \sqrt{\left(\frac{\delta q}{q}\right)^2 + \left(\frac{\delta \Delta P}{\Delta P}\right)^2} \quad (3.3)$$

A turbidity measurement unit estimates the fines concentration production. The accuracy of the turbidity measurement unit (δTM) is ±1 NTU (Nephelometric Turbidity Unit). Therefore, the uncertainty of the concentration of fines produced (δCFP) is given by the multiplication of turbidity measurement (TM) and the uncertainty of turbidity measurement, given by the turbidity measurement unit's accuracy. This relationship is presented in Equation 3.4.

$$\delta CFP = TM * \delta TM \quad (3.4)$$

Chapter 4 - Evaluation of SRT Facility Design for OHGP Applications

4.1. Introduction

The SRT facility was slightly modified for OHGP investigation, as presented in Chapter 3. This chapter evaluated the SRT facility design for OHGP application by performing a repeatability test and by replicating the operating parameters and materials used by Saucier (1974) to its available extension. For the testing parameters and materials not specified by Saucier (1974), Penberthy and Cope (1980) were used as a reference. Penberthy and Cope (1980) obtained results which support Saucier's findings. Therefore, it was considered a reference for the missing operating parameters and materials not found in Saucier's (1974) work. Different sets of data were recorded to validate the test with the results reported by Saucier (1974).

The replication of Saucier's operating parameters and materials allowed a comparison with Saucier's experimental work in terms of the trends for the produced particles and gravel-pack impairment. There was no expectation on matching the magnitude of the produced particles reported by Saucier (1974) since Saucier performed an investigation on one single perforation for CHGP completion while this research focused on a larger scale facility designed for OHGP.

The test repeatability is performed by repeating one of the tests under the same material and procedure. The data used for repeatability analysis consists of the differential pressure measurements across the cell and gravel-pack and the production of solid particles. The variability of the trends obtained for both tests is analyzed to conclude if the SRT facility can provide satisfactory test repeatability.

4.2. Testing Program and Materials

Saucier (1974) presents two different tests: one single PSD and two different gravel PSDs (Fig. 16). The two different gravel PSDs tested by Saucier (1974) corresponds to 20/40 and 16/30 US mesh, which D50s are 6.7 and 9.4 times larger than d50 of the PSD used for the tests replicated.

Therefore, a total of three tests are presented in this chapter. Tests 1 and 2 correspond to the 20/40 US mesh size and also account for the repeatability assessment. Meanwhile, Test 3 regards the 16/30 US mesh gravel size.

Concerning the load applied to the cell, an initial stage of the production is considered. Therefore, low stress on the gravel-pack is expected for an OHGP scenario (Bellarby 2009, Roostaei et al.

2018). The SRT cell's internal pressure can be about 60 psi for the highest flow rate during the test. Subsequently, the load applied to the cell during the tests is 120 psi. Although Saucier (1974) mentioned that mechanical load was applied on the sand-pack during the tests, the load magnitude was not provided.

Concerning salinity and pH, brine salinity of 25,000 parts per million (ppm) NaCl and pH of 7.9 were used for saturation and flow rates. The addition of NaCl occurs in deionized water. Brine salinity follows Penberthy and Cope's (1980) brine specifications. Saucier (1974) did not provide detailed information regarding the salinity for the injected brine.

4.3. Results and Discussion for Test Repeatability

Test repeatability is evaluating by comparing the variability between Tests 1 and 2. These tests were performed using the same procedure. The differential pressure for the cell top part (see Fig. 3-3) is presented in Figure 4-1. Differential pressures across the top part of the cell show a reasonable agreement, within 15% variability between the two data sets. The small variations in pressure drop may be attributed to small deviations when packing the sample. Since packing is performed manually, even though the same amount of mass is used per layer and the same load is applied on each layer by the consistent number of hits, the manual process is inevitably a source of error.

Differential pressure for both tests has an instant increase as flow injection starts. The pressure declines overtime, due likely to the fines migrating from the cell top toward the bottom. At minute 20, when the flow rate increases, the pressure drop has a sharp increase and tends to stabilize as the flow rate is kept constant. As differential pressure becomes constant, that is a clear indication that fines are no longer migrating from the cell's top part. In the final part of the test, at minute 45, the flow rate decreases to the initial flow rate, so differential pressure is instantaneity decreased and stabilized.

There is a significant oscillation in the differential pressure readings for the top part of the cell. The origin of this oscillation has been discussed in the previous chapter, and it occurs because the injection system did not provide steady flow injection. Tests 1, 2, and 3 were performed before the dampeners were added to the injection system.

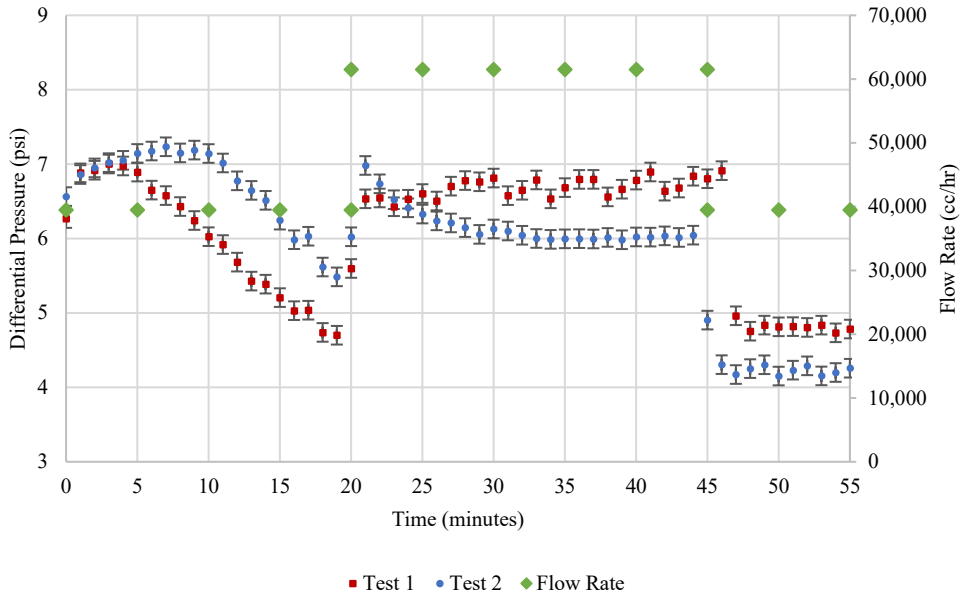

Figure 4-1. Differential pressure across the top part of the cell.

Figure 4-2 illustrates the differential pressure across the middle part of the cell. Differential pressures for the middle part of the cell show excellent agreement for both tests until minute 10, during which differential pressures increase with time. Until this moment, the middle part of the cell has been receiving more fines from the top part than releasing fines toward the bottom part. Between minutes 10 and 20, the pressure trends moderately deviate. While differential pressure for Test 1 continues to increase slightly, Test 2 presents a minor decrease followed by a stabilization in differential pressure. Within 10% variability between the two data sets, this small trend discordance may be related to the manual packing procedure. At minute 20, both tests show a sharp increase in differential pressure as the flow rate increases, followed by a decrease and further stabilization in pressure. It is noticed that the same trend seen previously for the top part of the cell is repeated for the middle part of the cell, except that for the middle part, stabilization takes a longer time since it will only occur once fines stop migrating from the top part. At minute 45, differential pressure declines and stabilizes instantly as the flow rate is reduced.

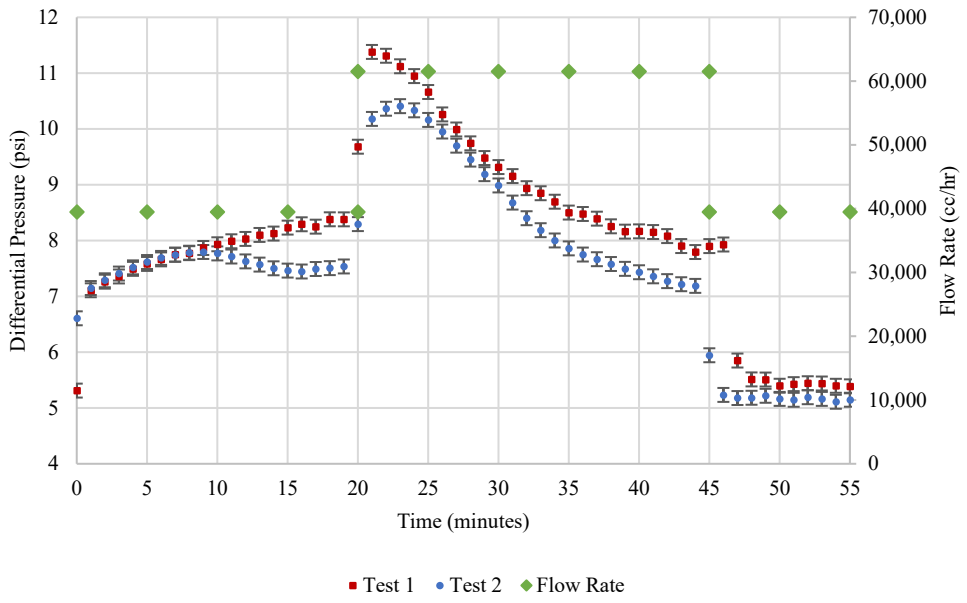

Figure 4-2. Differential pressure across the middle part of the cell.

Figure 4-3 displays the differential pressure across the cell's bottom part, including the formation sand and gravel interface. From the test initiation until minute 20, a continuous increase in pressure is registered due likely to the fines accumulation at the interface. The rate of fines migrating from both top and middle parts of the cell is considerably higher than the discharge rate through the interface, and consequently, through the gravel. As the flow rate increases at minute 20, a sharp increase is noticed as more fines are mobilized and keep getting accumulated at the formations and gravel interface. However, the trends start to change at a specific time for both tests when differential pressure decreases. The timing of this trend reversal is when the pressures at the cell top have stabilized- indicating little fines departure, and the middle part of the cell is also near stabilization. As little fines are migrating from the top and the middle, the cell bottom is losing fines from the gravel-pack, and fines concentration at the bottom decreases, hence, the lower pressure differentials. At minute 45, differential pressure declines as the flow rate is decreased. From that point to the end of the test, pressure decreases further, albeit at a lower rate as fewer fines are washed out due to the weaker drag forces created by the lower flow rate. The highest variability for differential pressure between the two data sets, within 20%, is registered at the highest flow rate.

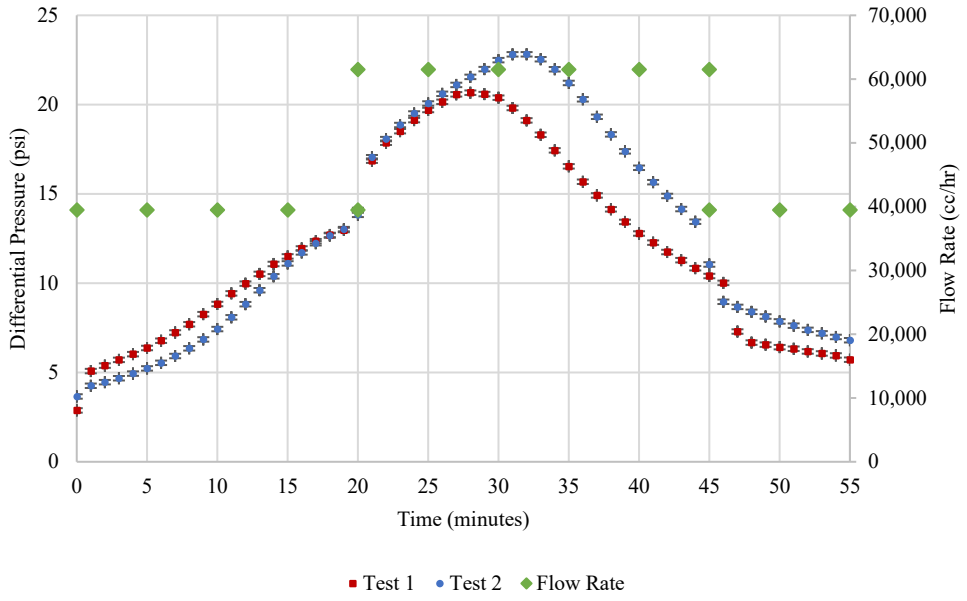

Figure 4-3. Differential pressure across the bottom part of the cell (interface).

Concerning the differential pressure across the gravel-pack, data is available only for Test 2 (Fig. 4-4). During Test 1, an operational issue caused unreliable data. Figure 4-4 shows stable differential pressures across the gravel-pack. From minute 10 to minute 20, a slight increase in differential pressure is correlated to fines accumulation inside the gravel-pack. It takes a bit of time for the pressure differentials to increase as the gravel has zero initial fines content. The sharp increase in pressure at minute 20 is due to the increase in flow rate. Consequently, more fines move into inside the gravel-pack. From minute 45 till the end of the test, the differential pressure decreases due to the lower flow rate but remains higher than the initial differential pressure even though the flow rate is the same. The differential pressure difference for the initial and final differential pressures is due to the permeability reduction and gravel-pack impairment.

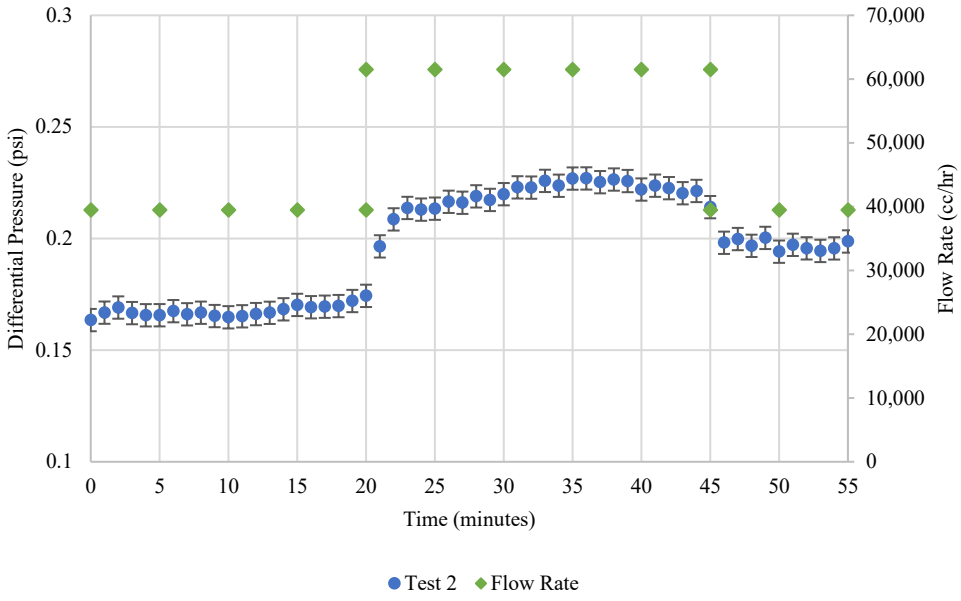

Figure 4-4. Differential pressure across gravel-pack.

The repeatability analysis of tests extended to the concentration of fines in the discharged water. Figure 4-5 presents the number of fines produced for both tests in intervals of 5 minutes. The low initial fines production is virtually constant for the first 10 minutes. From minute 10 until minute 20, an increase of fines production is observed. These initial low fines production followed by an increase is due to gravel invaded by fines, which occurs as fines start filling the gravel over time. Initially, the gravel is clean of fines, and fine particles start accumulating at the sand and gravel interface. The fine particles that pass the formation and gravel interface will either accumulate inside the gravel-pack structure or get produced. At minute 20, the flow rate is increased, and as expected, a higher quantity of fines is produced due to the higher drag forces. From minute 25 up to 45, the production of the fines decreases. After the initial shock caused by the increased flow rate, fines production tends to decrease and eventually stabilize at constant flow conditions. At minute 45, the flow rate is decreased to the initial flow rate and kept constant. For this interval, fines production is decreasing to reach low amounts.

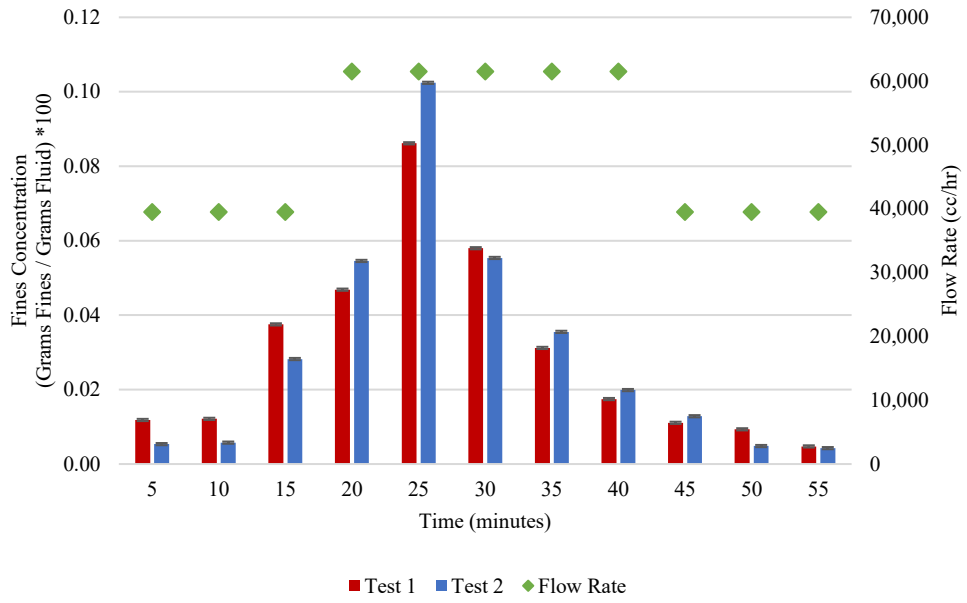

Figure 4-5. Produced fines.

Test measurements showed no sand production during the tests. All produced solids are smaller than 44 microns, which are classified as fines. Figure 4-5 compares the fines produced during Test 1 and Test 2, indicating good repeatability. The variability of the two data sets is higher at the initial and final timesteps, within 50%. The variability is reduced within 25% for the remaining timesteps. The variability recorded is likely due to the manual packing procedure. Despite the variability mentioned, the trends for produced fines for Test 1 and Test 2 are satisfactorily matched.

Another test measurement is the PSD of the produced fines for Test 2 by a laser PSD analyzer. The PSDs are presented for the three different flow-rate steps. Figure 4-6 presents the PSDs for the fines produced during the first flow stage, from minute 0 up to minute 20. Most particles produced during the first flow stage are tiny, within the range of 1-15µm.

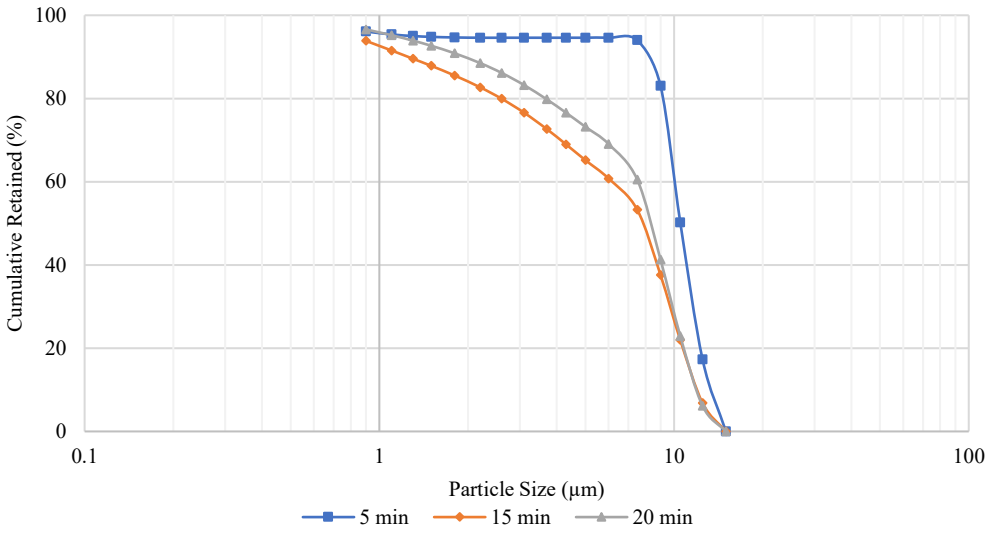

Figure 4-6. PSD of produced fines during the first flow stage of Test 2.

The PSDs of produced fines during the second flow stage (from minute 20 to 45) are shown in Figure 4-7. Most of the produced particles are within the range of 10-30µm, which are considerably coarser than the same during the first flow stage. Higher drag forces are created at a higher flow rate during the second flow stage, resulting in larger particles' production.

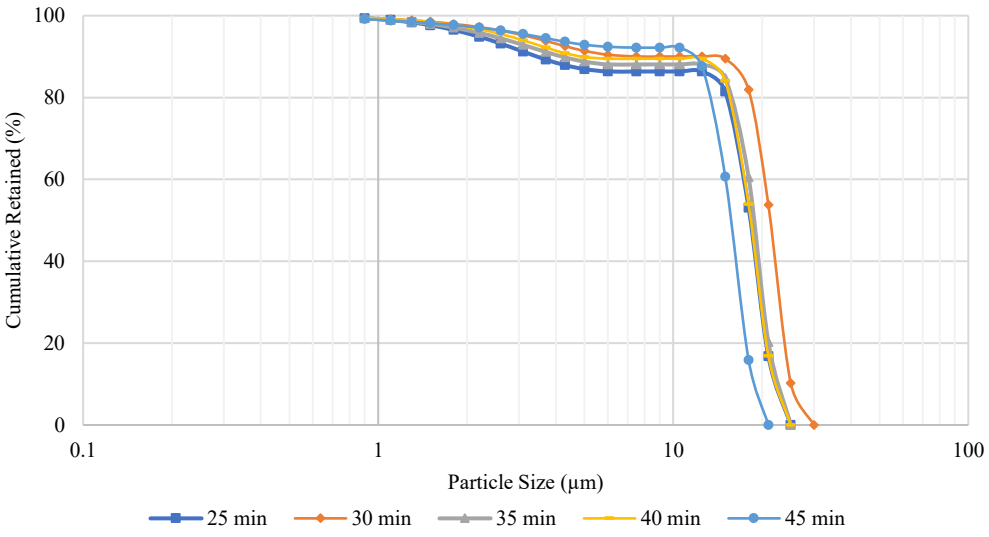

Figure 4-7. PSD for produced fines during the second flow stage of test 2.

The PSDs of the produced fines during the third flow stage (from minute 45 to 55) are plotted in Figure 4-8. The particle sizes are considerably variable for the two samples obtained during the third flow stage. It looks like the coarser fines in the first sample are the leftover from the previous

stage. Later, the fines sizes reduce to 5-15 microns, similar to what had been measured for the first stage.

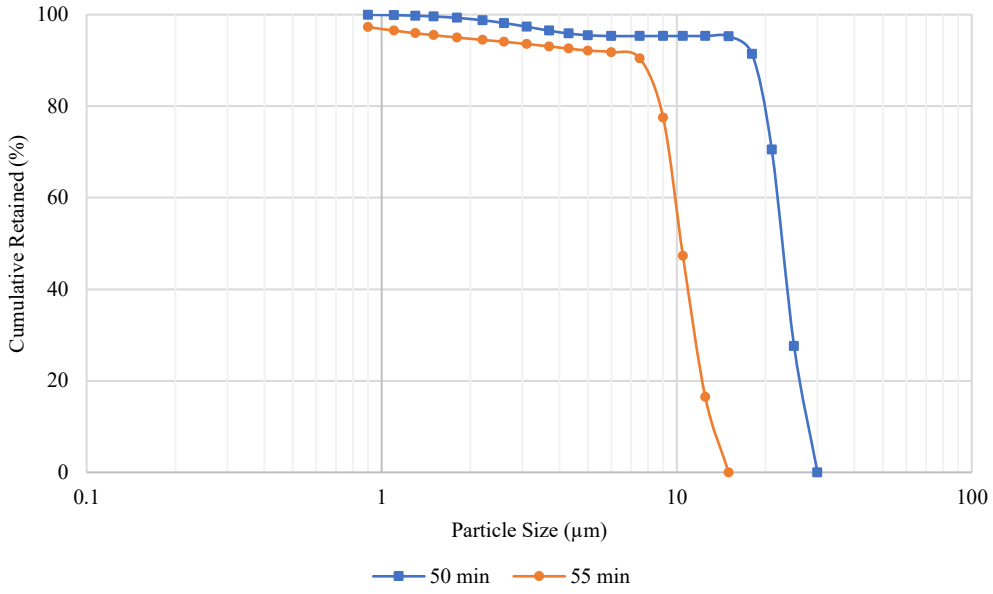

Figure 4-8. PSD of produced fines during the third flow stage of Test 2.

The assessment of pore throat size distribution was performed to compare the PSD of produced fines and the average pore throat size of both formation sand and gravel-pack. There are different methods available in the literature to calculate pore throat size. The correlation presented by Nabawy et al. (2009), Equation 4.1, was used to calculate the average pore throat size for the sand-pack and gravel-pack of Test 2. This correlation includes the porous media's permeability (K) and porosity (Ø) to obtain the average radius of pore throat size (r).

$$\log r = 0.603 \log K + 3.458 \log Ø - 6.277 \quad (4.1)$$

According to Nabawy's correlation, the average pore throat size of sand-pack and gravel-pack for Test 2 are 22 and 184 µm, respectively. Experiment research available in the literature (Barkman and Davidson, 1972; Van Oort et al. 1992) affirm that fine particles with the same size or larger than one-third of average pore throat size, tend to bridge at the entrance of pore throat. Meanwhile, fines smaller than one-third and larger than one-seventh of the average pore throat size tend to remain in the pore structure. The fines are easily produced if fine particles are smaller than one-fourteenth of the average pore throat size. Therefore, since the average pore throat size of sand-pack is 22 µm, according to the literature, most of the particles produced should be smaller than

1.5 µm. The justification for particles produced up to 30 µm is that the gravel was not washed before the test. It is reasonable to affirm that there are fine particles attached to the gravel particles which could be produced during the test. It is unknown the size of these fine particles presents in the gravel-pack structure before the test initialization.

4.3. Results and Discussion for Replication of Saucier (1974) Operating Parameters

This section presents a comparison between the results of tests 1, 2, and 3 and Saucier's (1974). Particle concentration and gravel-pack impairment are analyzed among Saucier's gravel-pack performance assessment (1974). Particle concentration is defined as the mass ratio of the particles produced and brine injected for a particular time step. Figure 4-9 presents the concentrations for tests 1, 2, and 3 and Saucier's experiment. For the first flow stage, from minute 0 to minute 20, the concentrations between tests 1, 2, and 3 and Saucier's experiment follow distinct trends. The likely reason for this disagreement is the absence of particles smaller than 10 microns in Saucier's experiment, which led to a faster sample stabilization in their test. Saucier (1974) registered a peak in concentration for the initial part of the test, which is probably due to an initial shock wave, followed by concentration decrease over time as the fines' production quickly stabilized. Test 3 displays a similar trend than Tests 1 and 2, although the number of fines produced by Test 3 is larger than the number of fines produced by Tests 1 and 2. This increase in concentration is expected once test 3 is performed with larger gravel. Consequently, the physical restriction created by the larger gravel structure is decreased, which leads to a higher concentration of fine particles produced.

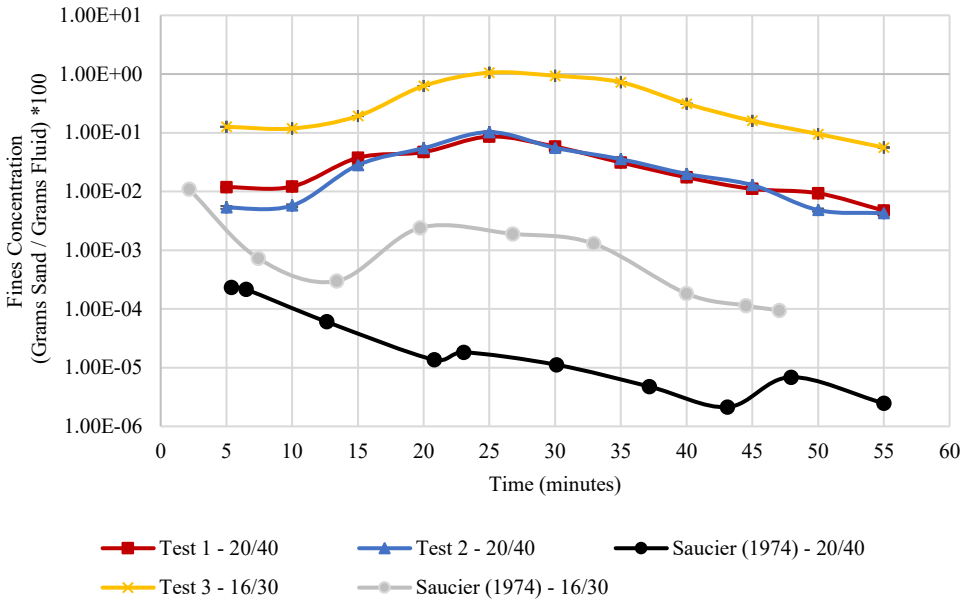

Figure 4-9. Comparison between the particle concentration in Saucier's experiment and current tests.

Figure 4-10 corresponds to the gravel impairment by fines accumulation in the gravel pore throats. Gravel impairment is determined as the ratio of final and initial gravel permeability versus the D50/d50 ratio, where D50 is the mean grain size for the gravel, and d50 is the same for the sand. The final permeability for Test 2 was 93% of initial permeability, while the final permeability for Saucier's experiment was 81% of initial permeability, where both cases have D50 of 6.7 times bigger than d50. In other words, gravel impairment for Test 2 was 7%, while gravel impairment for Saucier's 20/40 US mesh experiment was 19%. Meanwhile, the final permeability for Test 3 was 25%, and the final permeability for Saucier's 16/30 US mesh experiment was 28%. Therefore, the gravel-pack impairment for Test 3 was 75%, whereas the gravel-pack impairment for Saucier's 16/30 US mesh was 72%.

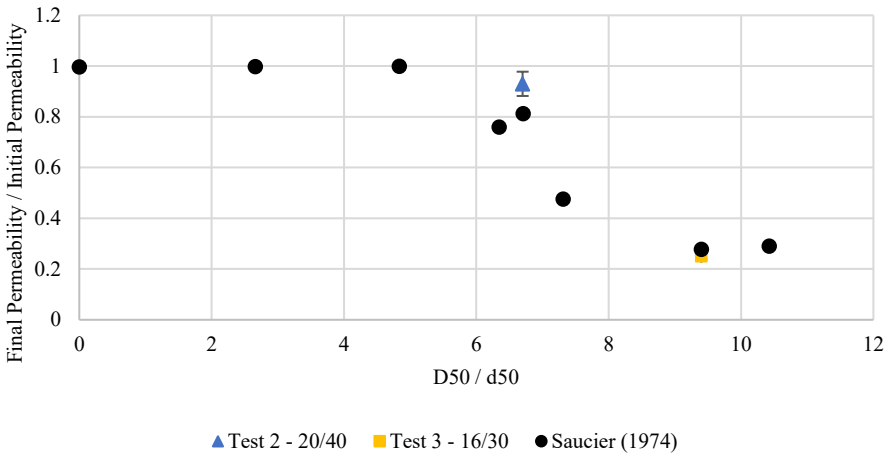

Figure 4-10. Comparison between the gravel-pack impairment in Saucier's experiment and current tests.

The difference in gravel impairment can be justified as (1) not all testing parameters for Saucier experiments were known for a full replication, and (2) the pressure ports in the SRT did not measure the pressure drop in the entire gravel-pack thickness. To elaborate further on the latter, the gravel-pack device has a total thickness of 2 inches, and the upper port is installed 0.3 inches below the sand-gravel interface (Fig. 4-11). As most of the gravel damage tends to occur close to the interface, most likely, the design used for ports location on gravel-pack design does not capture the total gravel damage generated by fines migration.

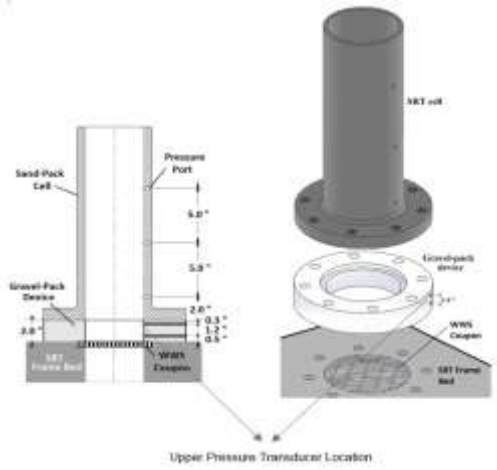

Figure 4-11. Distance of upper pressure transducer from the formation and gravel interface.

4.4. Conclusions

A large-scale SRT facility was slightly modified to investigate the open-hole gravel-pack design. Test repeatability was demonstrated by comparing the results from two different tests with the

same procedure. The SRT results were compared to the same from Saucier (1974) after replicating the testing parameters to the degree they were available.

Results indicate test repeatability for the presented SRT. The differential pressures across the cell present similar trends with minor deviations. The production of fines also demonstrates satisfactory alignment.

The differential pressure readings demonstrate the concept of fines migrating from the top part of the cell towards the bottom. The migration of fines leads to a decrease in differential pressure at the top part of the cell and increased differential pressure at the bottom due to fines accumulation. Eventually, the pressure drop at the sand and gravel-pack interface decreases as fines migration from the top and middle ceases, and the fines from the bottom part of the cell are washed out over time. Furthermore, some gravel-pack impairment is observed over time as some fines accumulate and remain inside the gravel-pack, slightly diminishing the initial gravel permeability.

A satisfactory agreement in the trends for the concentration of produced particles and the gravel-pack impairment boosts confidence in the SRT facility's ability and testing procedure for further gravel-pack research. Minor deviations in the concentration of produced fines in Saucier testing and the ones here are justified by excluding particles smaller than 10 microns in Saucier's experiments. Furthermore, the gravel-pack impairment obtained in the SRT is comparable to the same registered by Saucier (1974). Deviations are justified as the pressure port is placed at the optimum position at the sand-gravel interface.

Chapter 5 - Assessment of Saucier (1974) Gravel Sizing Criteria for Highly Non-Uniform and High Fines Content Formations and Salinity Level Variation

5.1. Introduction

Most of the gravel-pack literature refers to gravel-pack well preparation and techniques for improving and achieving satisfactory gravel placement. Although the literature on gravel-pack design is existent, it is not as extensive. Therefore, gaps in the literature may be addressed to understand further the limitations of the current gravel sizing design criteria used by the oil and gas industry.

The gravel sizing criteria proposed by Saucier (1974), currently used by the industry, has been developed on a formation with UC of 3.6. Penberthy and Cope (1980) further investigated the gravel-pack design criteria, proposed by Saucier (1974), for two formations with UC equals to 1.5 and 3.6. Both studies obtained satisfactory gravel-pack performance for the sizing range of D50 equals 5-6x d50. However, since OHGP is an appropriate alternative for poorly sorted sands with high fines content, and as formations with UC considerably higher than 3.6 are commonly seen, these features should be integrated into the gravel-pack assessment design.

Furthermore, there is no literature available on how salinity level may impact the gravel-pack performance. For scenarios that englobe a formation with high UC, therefore less stability of the sand arch around the formation and gravel interface, and high fines content, the salinity level may directly affect the number of fines carried towards the well. The number of fines detaching from the formation grains and moving in the direction of the well may impact the gravel-pack performance in case gravel sizing is not adequately designed.

This chapter assesses Saucier's (1974) design criteria for formations with a high fine content amount, higher than 10%, and highly non-uniform, UC higher than 10. Furthermore, the analysis of how salinity variation may impact the gravel-pack performance is also performed. Therefore, evaluating gravel sizing criteria for formations with these features allow the further understanding of the limitations of Saucier's (1974) design criteria for gravel sizing.

The assessment of Saucier's gravel sizing criteria is performed by analyzing the pressure drop build-up at the formation and gravel interface and the gravel-pack impairment. These evaluation criteria enable the clarification of how effectively Saucier's gravel sizing can handle the

accumulation of fines at the formation and gravel interface, related to productivity loss. Furthermore, the gravel impairment provides information on the intensity of gravel-pack plugging.

5.2. Testing Program and Materials

The PSD 1 (see Fig. 3-5) was selected for this investigation. PSD 1 presents a UC of 12 with 12% of its particles being accounted for fine particles (smaller than 44 microns), which satisfies both requirements proposed for the PSD selection. The commercial sand recipe used for matching PSD 1 is presented in Table 4-2. The gravel PSD, 12/16 US mesh, is presented in Figure 3-5. The D50 is 5.64 times larger than d50, therefore within Saucier (1974) sizing criteria.

The test matrix proposed is shown in Figure 5-1. While the formation and gravel PSD are kept the same for all the tests performed, the salinity level varies. Tests 6 and 7 have the same salinity level since Test 7 was performed to replicate Test 6 to account for the testing variability.

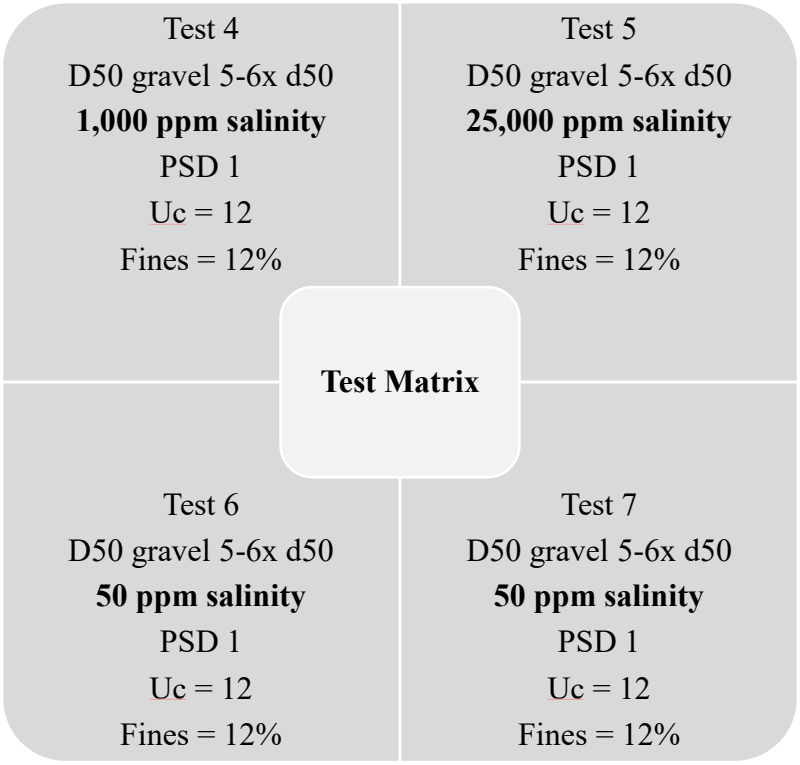

Figure 5-1. Text matrix for the assessment of Saucier (1974) design criteria.

The salinity level of 1,000 ppm of NaCl was proposed as a lower bound for salinity investigation based on a data set published, in 2002, by the U.S. Geological Survey. Salinity levels lower than 1,000 ppm are not expected for conventional wells. Therefore, 1,000 ppm salinity level is

considered as the realistically worst-case scenario for conventional wells. However, the hypothetically worst-case scenario would be 50 ppm, as this corresponds to the highest zeta-potential (Fig. 2-11), and consequently, the highest dispersion (Fig. 2-12) for clay particles. Then, 50 ppm salinity level was included in the test matrix to assess Saucier's (1974) design criteria for the possible worst-case scenario for fine particles release. Although it is relatively common to find salinity levels higher than 25,000 ppm for conventional wells (U.S. Geological Survey, 2002), 25,000 ppm NaCl was selected as the upper bound. The selection of the upper bound salinity level is justified because 25,000 ppm NaCl was the salinity used during the experiments performed by Penberthy and Cope (1980), which matched Saucier's outcome (1974).

Table 5-1 below, displays the zeta potentials for the salinity levels used in the test matrix and their corresponding dispersion zone. While salinity level of 50 ppm presents a solid good dispersion behaviour, 1,000 and 25,000 ppm salinity levels present similar zeta potential values. However, 1,000 ppm salinity level is in the initial moderate dispersion zone while 25,000 ppm salinity level is in the incipient flocculation zone (see Fig. 2-12).

Table 5-1. Zeta potential for each salinity level and their corresponding dispersion zone.

Salinity (ppm)	Zeta Potential (mV)	Dispersion Zone
50	-52	Good dispersion
1,000	- 32	Initial moderate dispersion
25,000	- 28	Incipient flocculation

Regarding the flow rates, three different flow stages were designed for the test matrix previously presented. The flow rates were estimated considering the flux rate calculation for a set of OHGP wells for various field cases. The flux rates were then distributed in low, intermediate, and high. The flow rates were calculated by scaling the three flux rates to the coupon area of WWS used for the tests (Fig. 3-8). The load applied to the cell during the test matrix tests (Tests 4, 5, 6, and 7) was 120 psi.

5.3. Fines Migration for Low Flow Rate - Flow Stage 1

Since the drag and electrostatic forces play essential roles in the attachment and detachment equilibrium of fine particles during flow conditions, a modification in the initial fine particles condition may occur depending on the balance between these two primary forces (Aji, 2014). Therefore, considering the constant flow rate during each flow stage, it is possible to analyze how the salinity level variation impacts the fines mobilization.

Figure 5-2 displays the differential pressure across the top part of the cell for the four tests performed during the low flow rate injection (11 L/hr). The initial differential pressure peak is attributed to both brine injection and the consequent fine particles mobilization. Tests 6 and 7 (Fig. 5-2) present the lowest differential pressure for the top part of the cell than Tests 4 and 5. This behavior matches the expectation once a low salinity level leads to decreased electrostatic forces between fine particles and formation particles. Therefore, more fine particles are in dispersion for Test 6 and 7, and these particles are easily carried away from the top part of the cell. A lower quantity of fine particles in the top part of the cell results in lower differential pressures registered for both Tests 6 and 7. It is possible to observe that Tests 6 and 7 have similar differential pressure readings with minimal variation beyond the error estimation. The average variability registered between Tests 6 and 7 is 16%. This variation beyond the error estimation is most likely due to the packing procedure, which is a manual procedure and is a source of error.

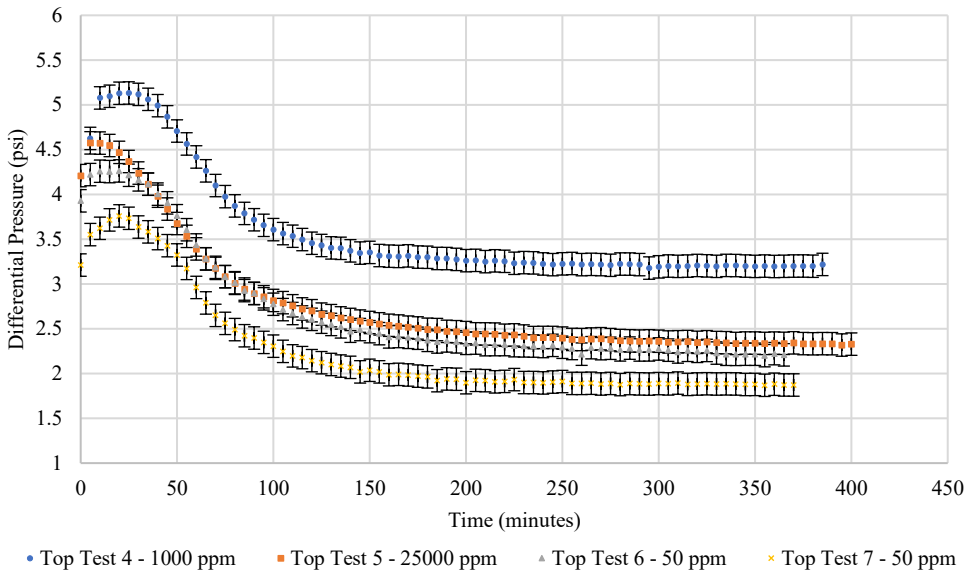

Figure 5-2. Differential pressure across the top part of the cell for low flow rate (flow stage 1).

Tests 4 and 5 present differential pressure results that differ from the statement made above regarding the salinity level and the consequent attachment and detachment of fines (see Fig. 5-2). As Test 5 (25,000 ppm) presents a higher salinity level than Test 4 (1,000 ppm), the expectation was that the differential pressure across the top part of the cell for Test 5 should remain higher than for Test 4. Due to the higher salinity level, higher electrostatic forces are expected to occur for Test 5, and, therefore, fewer fines should detach from the formation particles. The hypothesis for the deviation seen is that the packing procedure, although systematically and consistently performed, introduces a human error source. The packing procedure is an error source challenging to account for individually, and it generates inevitable variability that can lead to inconsistency in the data collected. Estimation of error accounted to packing procedure would require additional tests following the same procedure and material.

Figure 5-3 presents the differential pressure for the middle part of the cell during the first flow stage. It is possible to see the same behavior previously pointed out for the top part of the cell in differential pressure and fines migration. The significant difference is that the middle part of the cell shows a peak in differential pressure at a later time window when compared to the top part. This shift in time happens because, in the beginning, the middle part is initially receiving more fines from the top than it is releasing toward the bottom. Then, by the point where the top part starts releasing fewer fines, heading to stabilization, the middle part releases more fines to the

bottom than it is receiving from the top part of the cell. Consequently, by this point, the differential pressure starts decreasing.

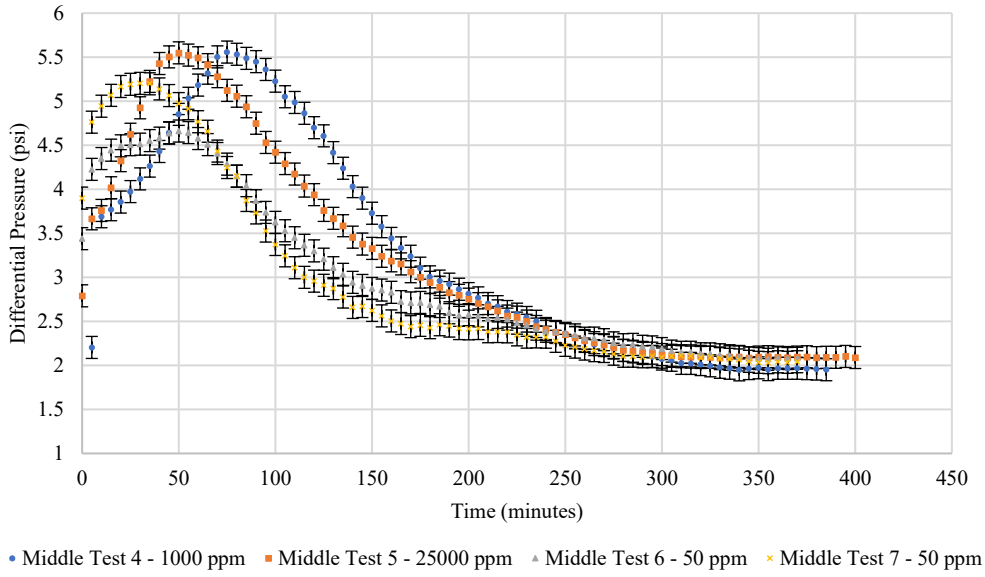

Figure 5-3. Differential pressure across the middle part of the cell for low flow rate (flow stage 1).

Figure 5-4 displays the differential pressure across the formation and gravel interface for the first flow stage. The differential pressure achieves a higher peak compared to the previous top and middle sections of the cell. The higher differential pressure occurs in the bottom part due to the accumulation of fine particles at the formation and gravel interface. As the rate of fines received from both top and middle parts of the cell is higher than the rate of fines able to move through the formation and gravel interface, this accumulation occurs. A slightly higher peak in differential pressure happens in Tests 6 and 7, which matches the expectation of a higher quantity of fines accumulating at the formation and gravel interface. This phenomenon occurs since a lower salinity level leads to fine particles detachment and higher mobilization of fines. Eventually, when the fine particle mobilization starts stabilizing for the top and middle parts of the cell, it is possible to see a decrease in differential pressure for the interface. This decrease behavior is a washout process sustained until both differential pressure and production of fines stabilize entirely.

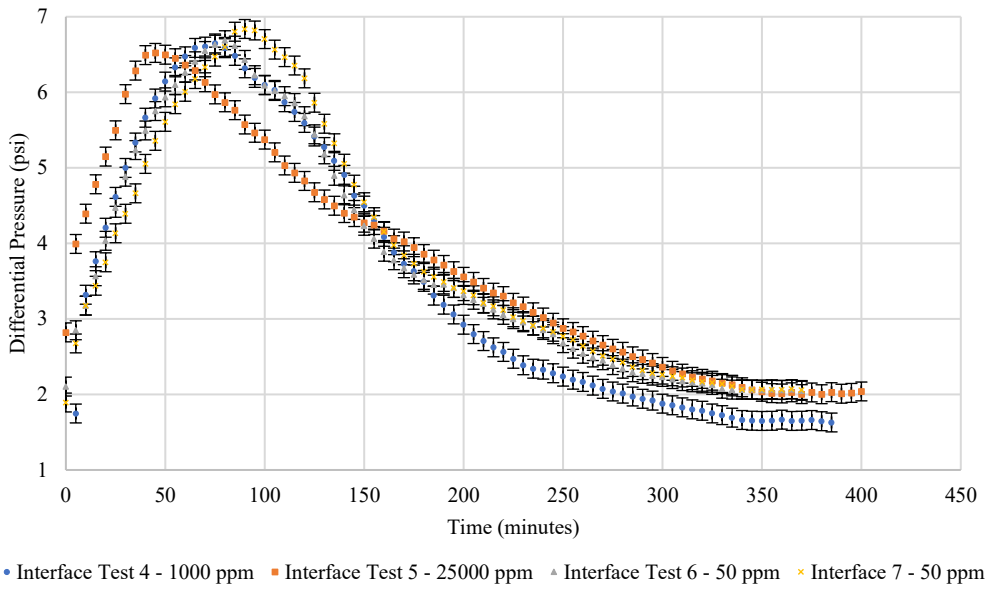

Figure 5-4. Differential pressure across the bottom part of the cell (interface) for low flow rate (flow stage 1).

Figure 5-5 shows the differential pressure across the gravel-pack structure for the first flow stage. The upper and lower error boundaries, represented in black markers, are displayed instead of error bars for better visualization as the error bars would overlap each other. For the first 15 minutes, a subtle increase in the differential pressure inside the gravel-pack structure is seen. As explained in the previous chapter, initially, the gravel-pack is free of fines, and as brine is injected through the gravel structure, fines start filling up the originally fines free gravel-pack pore throats. As the brine injection persists, the fine particles keep entering the remaining spaces in the gravel-pack and, therefore, a slight increase in pressure occurs. Since more particles are mobilized for Tests 6 and 7, it is possible to see a higher differential pressure for these tests. The higher the number of fine particles moved throughout the gravel-pack structure, the higher is the number of fines expected to accumulate inside the gravel-pack. Consequently, the differential pressure for Tests 6 and 7 is higher than for Tests 4 and 5 (see Fig. 5-5). Although, when accounting for the uncertainty analysis displayed by the error bars in Figure 5-5, the differential pressures registered for Tests 4, 5, 6, and 7 are similar and overlap each other.

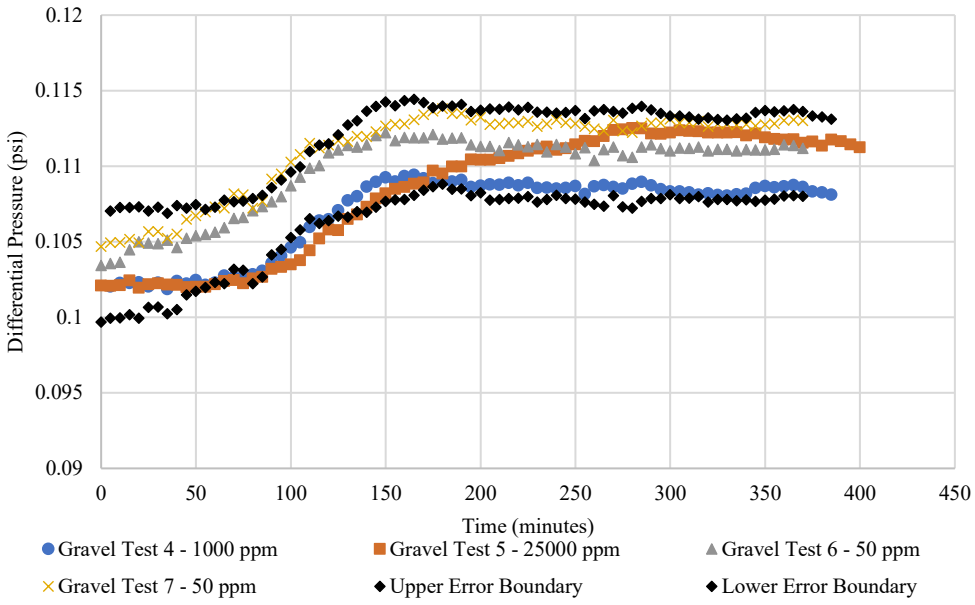

Figure 5-5. Differential pressure across the gravel-pack structure for low flow rate (flow stage 1).

Table 5-2 displays the gravel-pack's initial permeability and the permeability measurement for the gravel-pack structure after the first flow stage. A reduction in the permeability is seen for all the tests as fine particles move inside the gravel-pack structure plugging the pore throats. A similar amount of permeability decrease is registered for the four tests despite the salinity level difference.

Table 5-2. Permeability measurement for the gravel-pack structure before and after flow stage 1.

Test Number	K Before Flow Stage 1 (D)	K After Flow Stage 1 (D)
Test 4	60.0	58.5
Test 5	60.0	57.8
Test 6	60.0	58.0
Test 7	59.8	57.5

5.4. Fines Migration for Intermediate Flow Rate - Flow Stage 2

Regarding the second flow stage, Figure 5.6 displays the differential pressure across the top part of the cell for the four tests performed during the intermediate flow rate (48 L/hr). The initial

differential pressure peak for the top part of the cell is less sharp than the peak registered for the cell's top during the first flow stage. This difference occurs since, most likely, the majority of the fines mobilization for the top part of the cell happened during the first flow stage. Albeit some fines are mobilized still during the second flow stage, as a slight decrease followed by stabilization is registered for all the top part of the cell tests. Tests 6 and 7 present the lowest differential pressure readings once the electrostatic forces are weaker for the salinity level of 50 ppm. Tests 4 and 5, on the other hand, show higher differential pressure readings as fewer fines are mobilized toward the bottom part of the cell.

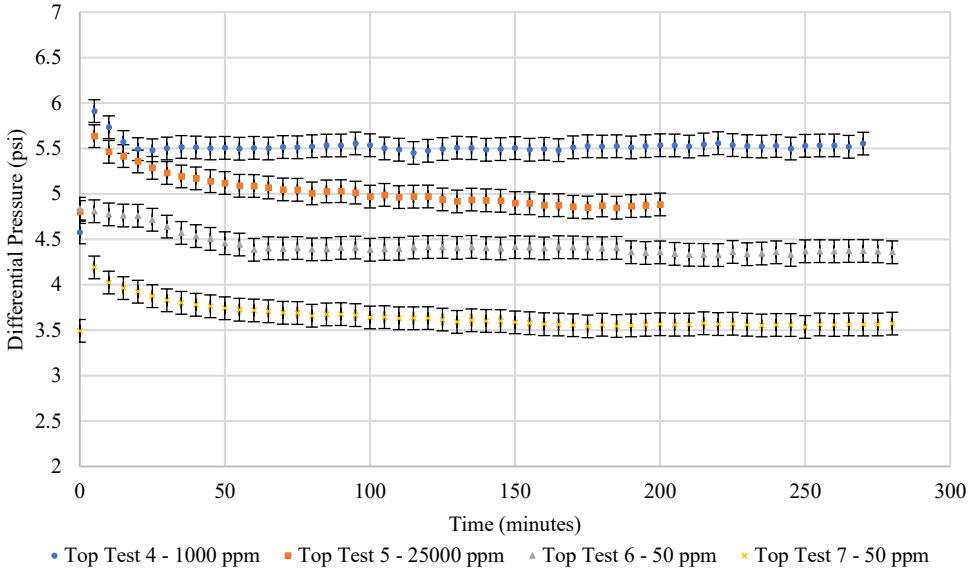

Figure 5-6. Differential pressure across top part of the cell for intermediate flow rate (second flow stage).

Figure 5-7 presents the differential pressure readings for the middle part of the cell for the second flow stage. The differential pressure declines overtime for all the tests until stabilization occurs. Once the release of fine particles from the top part ceases in the early part of the second flow stage, the middle part of the cell loses fine particles. Consequently, the middle part's stabilization takes a longer time than for the top part of the cell.

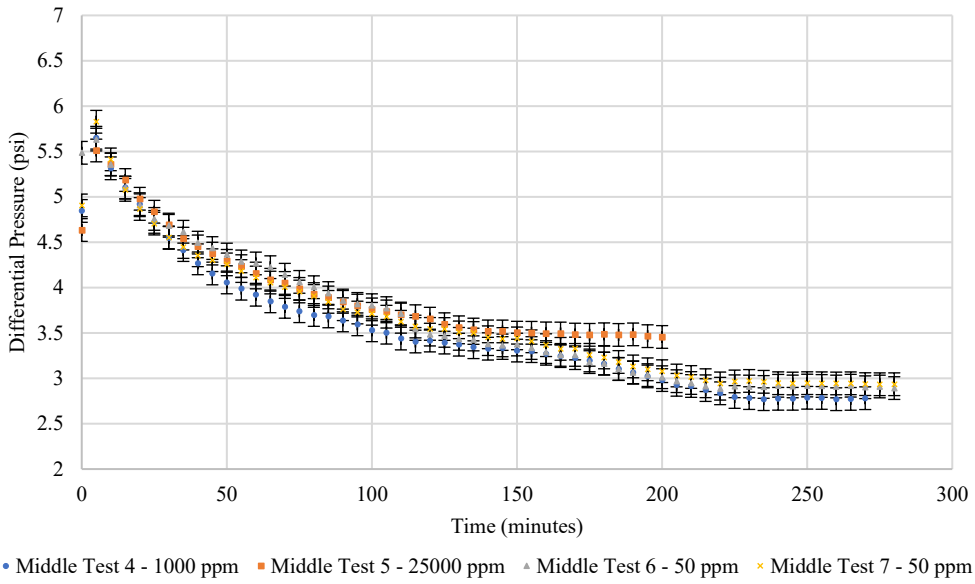

Figure 5-7. Differential pressure across middle part of the cell for intermediate flow rate (second flow stage).

Figure 5-8 shows the interface differential pressure readings for the second flow stage. As the accumulation of fines is more accentuated at the formation and gravel-pack structure, higher differential pressures are registered due to the bridging phenomenon. Tests 6 and 7 display higher differential pressure readings when compared to Tests 4 and 5. This difference is experienced because a lower salinity level leads to higher detachment and dispersion rates of fines from the formation particles. Consequently, a higher quantity of fines is mobilized toward the cell interface during Tests 6 and 7, plugging the pore throats more effectively and increasing the localized pressure drop.

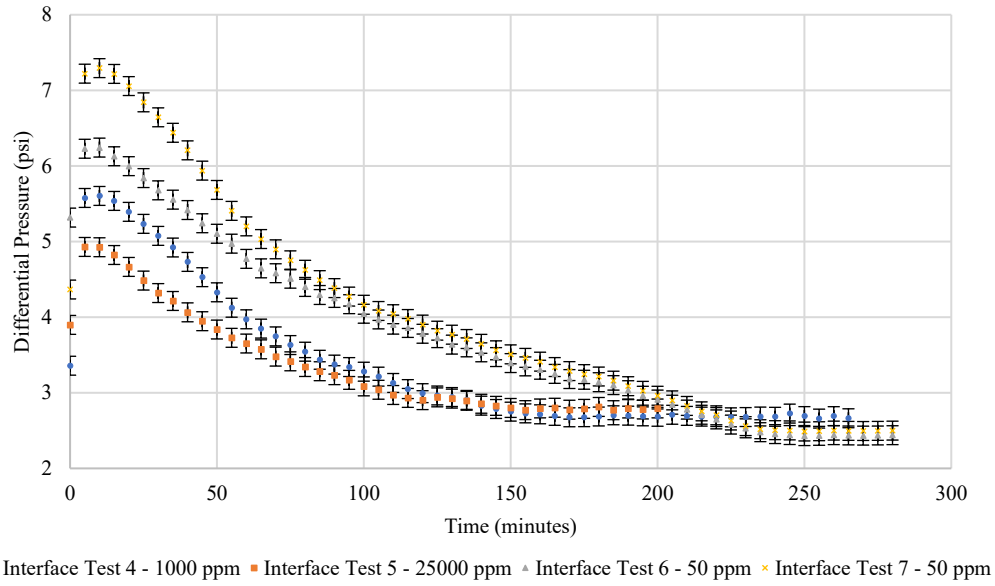

Figure 5-8. Differential pressure across bottom part of the cell (interface) for intermediate flow rate (second flow stage).

Figure 5-9 shows the differential pressure readings for the gravel-pack in the second flow stage. The higher differential pressure registered for both Tests 6 and 7 reveals that gravel-pack permeability impairment is higher for these two tests than Tests 4 and 5. This additional differential pressure is justified by the higher quantity of fine particles remaining inside the gravel-pack structure. As a higher concentration of fines is being mobilized toward the gravel-pack structure during tests performed with low salinity level, more likely to fines accumulate inside the gravel-pack and plug its pore throats more effectively.

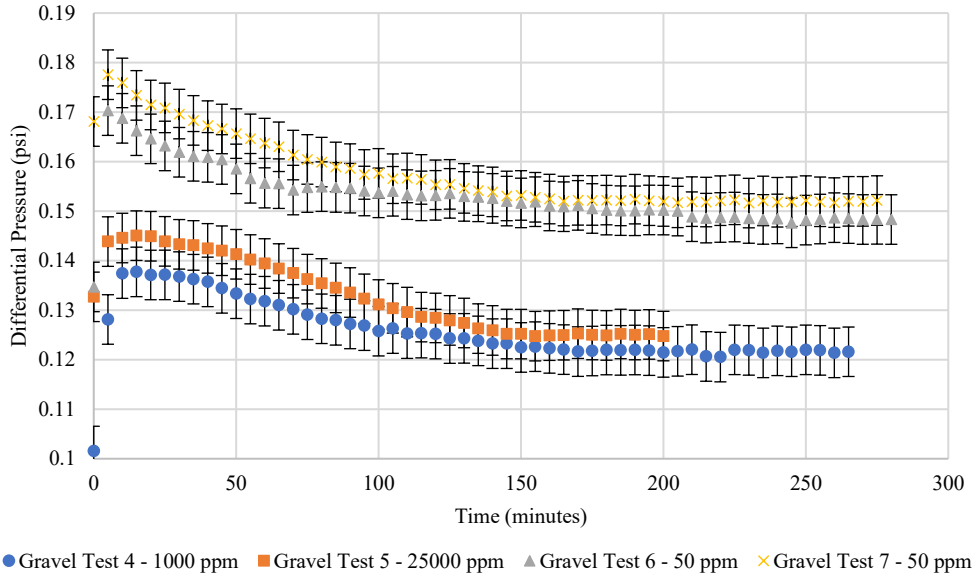

Figure 5-9. Differential pressure across gravel-pack for intermediate flow rate (second flow stage).

Table 5-3 shows the permeability measurement for the gravel-pack structure before and after the second flow stage. A further reduction in the permeability is registered for all the tests as a higher number of fine particles move inside the gravel-pack structure. Because of higher drag forces generated during the second flow stage, more fines are mobilized inside the gravel-pack structure compared to the first flow stage. Therefore, permeability is further reduced by the end of the second flow stage. Tests 6 and 7 present the highest gravel-pack impairment due to the low salinity level. The low salinity leads to weaker bonding forces among fine particles, allowing higher fines mobilization towards the gravel-pack.

Table 5-3. Permeability measurement for the gravel-pack structure before and after flow stage 2.

Test Number	K Before Flow Stage 2 (D)	K After Flow Stage 2 (D)
Test 4	58.5	55.5
Test 5	57.8	55.2
Test 6	58.0	40.0

Test 7	57.5	36.0

5.5. Fines Migration for High Flow Rate - Flow Stage 3

Regarding the last flow stage, Figure 5-10 presents the differential pressure recordings for the top part of the cell for the high flow rate (112 L/hr). Albeit the flow rate for the third flow stage is considerably higher than for the previous two flow states, a slight peak in pressure is seen, and the differential pressure stabilizes quickly for the four tests. This quick pressure stabilization happens because not many mobile fine particles are available in the cell's top part after the first and second flow stages are concluded. Once again, Tests 6 and 7 present the lowest differential pressures since more fine particles have been displaced for these tests due to the low salinity level of 50 ppm.

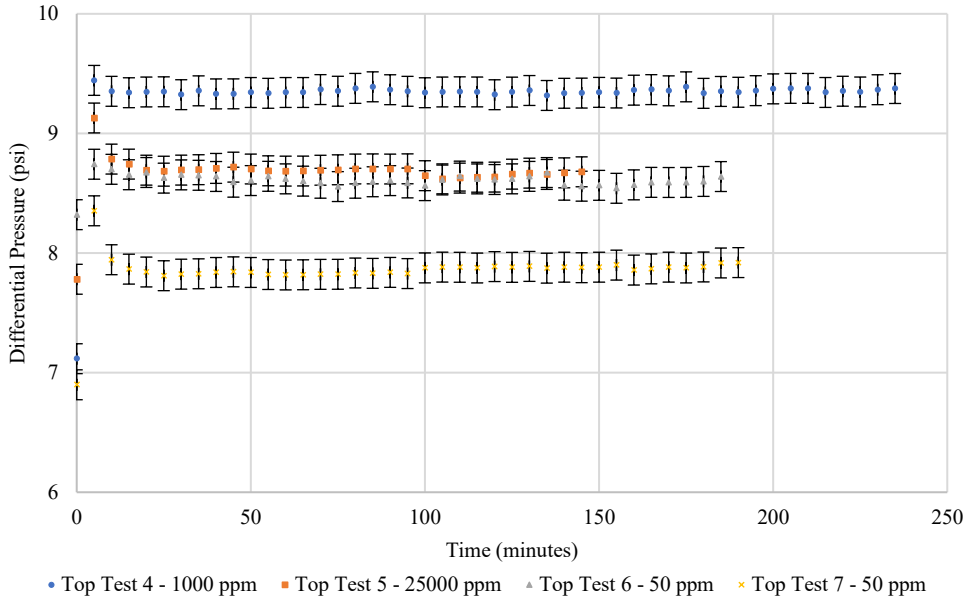

Figure 5-10. Differential pressure across top part of the cell for high flow rate (third flow stage).

Figure 5-11 displays the differential pressure across the middle part of the cell for the third flow stage. As the middle part of the cell receives the fine particles from the top and release fines toward the bottom, it becomes the most challenging part of the cell to drive to a conclusion. Tests 4, 6, and 7 follow the same fast stabilization behavior, while Test 5 takes longer to stabilize fully.

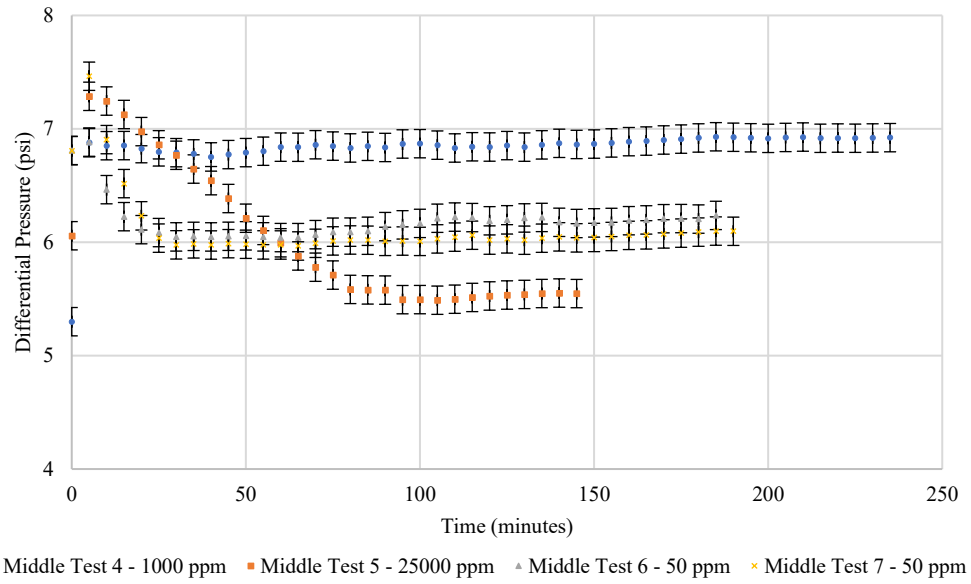

Figure 5-11. Differential pressure across middle part of the cell for high flow rate (third flow stage).

Figure 5-12 shows the differential pressure for the bottom (interface) part of the cell. As the stabilization for the top and middle part of the cell is reached, the fine particles are no longer displaced from the top and middle toward the bottom part. Therefore, the accumulation of fine particles at the formation and gravel interface decreases by the washout process of fine particles. Tests 6 and 7 present higher differential pressure at the beginning of the third flow stage as more fine particles are mobilized due to the low salinity level. Then, these fine particles accumulate at the formation and gravel interface, increasing the differential pressure. Although the gravel sizing used seems to provide a higher pressure build-up for low salinity level tests, the washout process is not jeopardized over time, and in fact, the differential pressure at the interface is lower for Tests 6 and 7 when compared to Tests 3 and 4, by the end of the third flow stage.

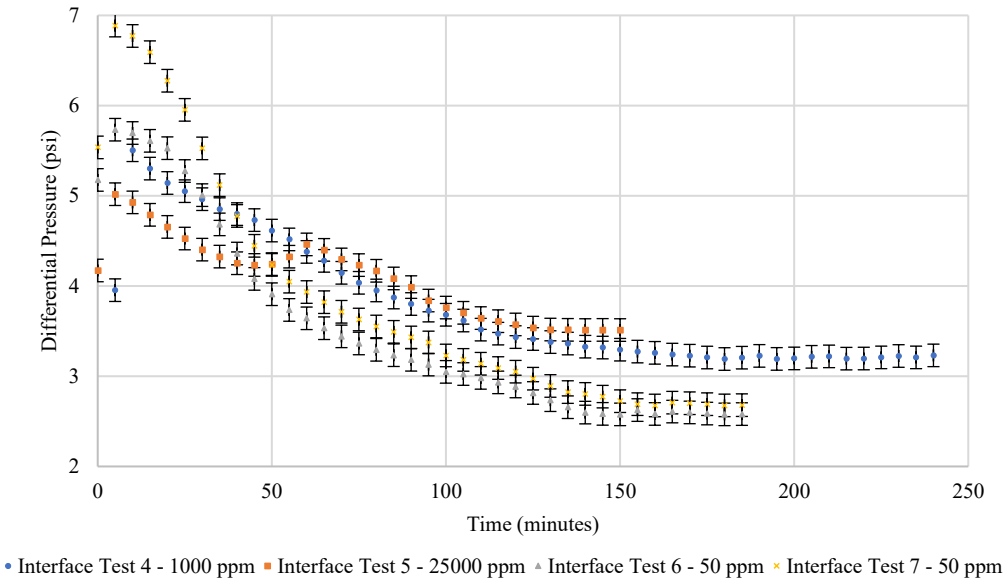

Figure 5-12. Differential pressure across bottom (interface) part of the cell for high flow rate (third flow stage).

Figure 5-13 displays the differential pressure readings for the gravel-pack structure in the third flow stage. Tests 6 and 7 present higher differential pressures in the gravel-pack porous media as more fine particles are dispersed and mobilized toward the gravel during low salinity tests. These fine particles are not thoroughly washed out from the gravel, which leads to the permeability reduction of the gravel-pack structure. Tests 4 and 5 seem to have virtually the same differential pressure, indicating that not much difference in the number of fines remaining inside the gravel structure occurs. The gap in differential pressure from Tests 4 and 5 to Tests 6 and 7 shows that as more fines reach and penetrate the gravel-pack structure, higher is the gravel-pack impairment caused by the accumulation of fines inside the gravel structure. Although Tests 4 and 5 have very distinct salinity levels, the differential pressure readings suggest that the drag forces generated by the flow rates applied are playing the primary role in the mobilization of fine particles for both Tests 4 and 5. Consequently, despite the higher electrostatic forces generated for Test 5 (25,000 ppm salinity), the drag forces are high enough to mobilize those fines as much as for Test 4 (1,000 ppm salinity).

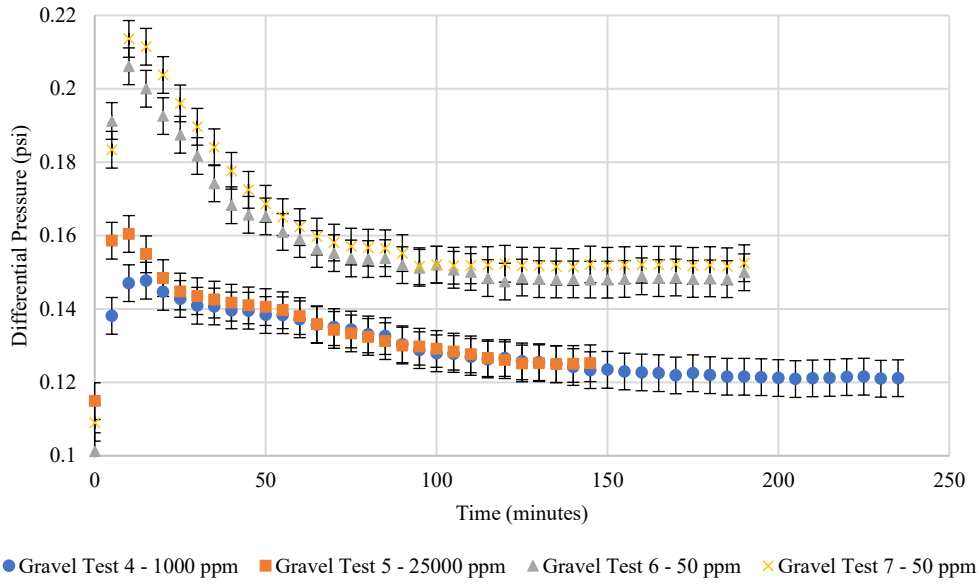

Figure 5-13. Differential pressure across gravel-pack for high flow rate (third flow stage).

Tests 6 and 7 show a steep slope in differential pressure decrease for the first 50 minutes (Fig. 5-13). The flow rate for the third flow stage (112 L/hr) is considerably higher than for the previous two flow stages (11 and 42 L/hr). As there is an abrupt change in flow velocity, this initial agitation develops pressure disturbance in the gravel-pack and, consequently, a high amount of fine particles are carried away. This pressure disturbance most likely contributes to washing out fine particles from the gravel-pack structure.

Table 5-4 presents the permeability measurement for the gravel-pack structure before and after the third flow stage. At this point, a further reduction in the permeability would be expected for all the tests as more fines would move inside the gravel-pack structure due to even higher drag forces experienced during the third flow stage. However, a slight increase in the gravel-pack permeability is seen for the four tests. The justification for such output is that the SRT facility provides a limited amount of fines in the porous sample. Therefore, most of the mobile fines present in the sand-pack cell have been mobilized towards the gravel-pack structure during the first two flow stages. Although the drag forces generated during the third flow stage are high, not much mobile fines are present in the sand-pack cell at this point. Figures 5-10 and 5-11 show that stabilization occurs quickly for both the cell's top and middle parts.

Meanwhile, Figure 5-12 ensures that fines are still moving from the bottom part of the cell towards the gravel-pack. However, the steep differential pressure in Figure 5-13 shows that a considerable amount of fines produced during the third flow stage comes from the gravel-pack structure. This point is inconsistent once under field conditions, fines from the well vicinity would most likely be mobilized towards the well due to higher drag forces. Consequently, a higher gravel-pack impairment would be expected after the third flow stage.

Table 5-4. Permeability measurement for the gravel-pack structure before and after flow stage 3.

Test Number	K Before Flow Stage 3 (D)	K After Flow Stage 3 (D)
Test 4	55.5	57.5
Test 5	55.2	56.5
Test 6	40.0	42.0
Test 7	36.0	39.6

5.6. Fines and Sand Production

During the tests performed for this research, no sand production has been reported. Therefore, all the particles which entirely passed through the grave-pack structure and were produced were larger than 44 microns.

Figure 5-14 displays the fines concentration measurements and total fines production for the first flow stage (low flow rate). The initial 15 minutes present a stable fines concentration due to the initial free fines gravel-pack condition. As the fines fill-up the gravel-pack structure, the produced fines concentration rises, which starts around minute 20. From minute 20, a sharp increase in fines concentration occurs until a peak is reached for all the tests. Once the peak production of fine particles occurs, a decline followed by a stabilization trend is registered in all the tests. The fines concentration keeps reducing over time as the fine particles are washed out from the formation and gravel interface, and the migration of fines from both top and middle parts stabilize. Eventually, the same happens to the bottom part of the cell and, consequently, both differential pressures across the cell and gravel-pack structure, as well as the fines concentration, fully stabilizes. Figure 5-14

shows the stabilization period for each test. At least 3 PV were injected as stabilization criteria for the first flow stage. The criteria for stabilization were considered as differential pressure and fines concentration to be fully stabilized for at least 3 PV injected.

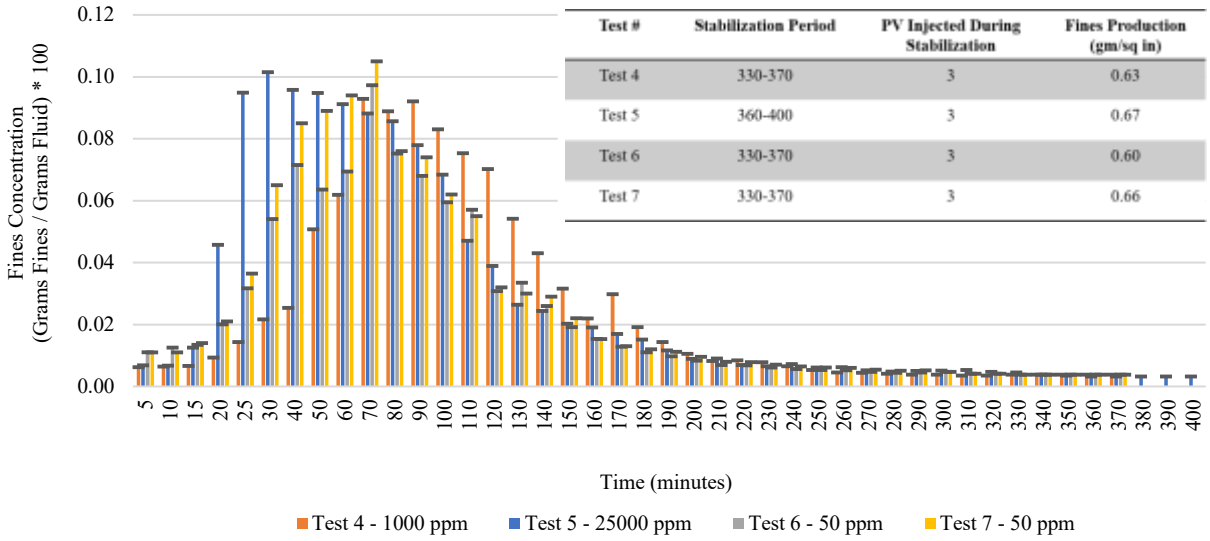

Test #	Stabilization Period	PV Injected During Stabilization	Fines Production (gm/sq in)
Test 4	330-370	3	0.63
Test 5	360-400	3	0.67
Test 6	330-370	3	0.60
Test 7	330-370	3	0.66

Figure 5-14. Fines production for low flow rate (first flow stage).

Figure 5-15 displays the produced fines concentration and total fines production for the second flow stage (intermediate flow rate). Tests 6 and 7 present the peak of fines concentration for the first few time-steps. This peak in fines concentration happens due to the combination of abrupt change in flow velocity with the high amount of fines in dispersion due to the low salinity level for Tests 6 and 7. This combination causes an instant release of fines by pressure disturbance of the porous media.

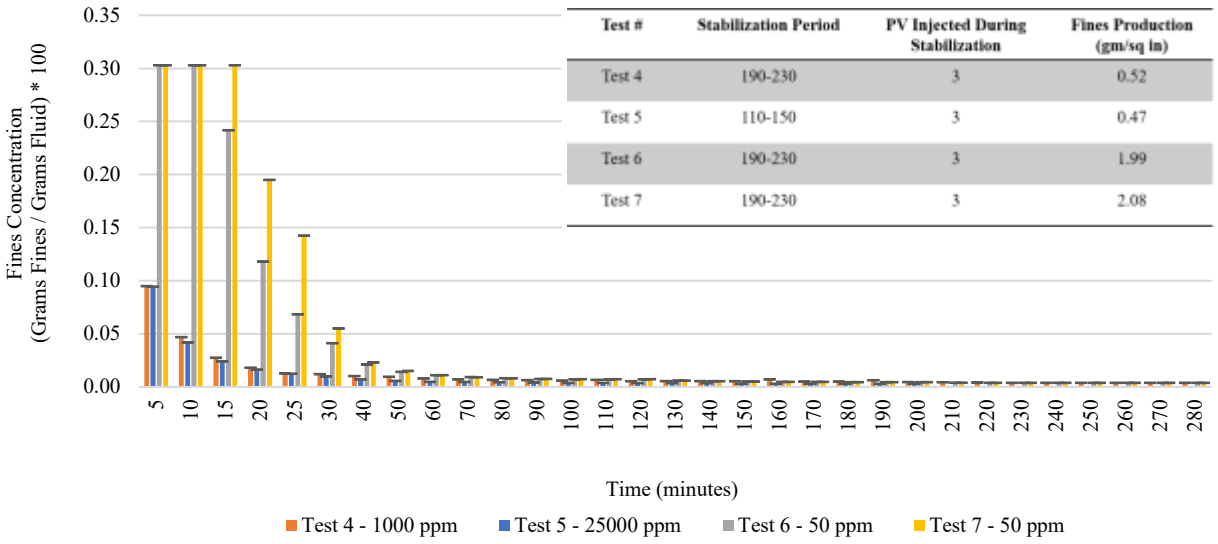

Test #	Stabilization Period	PV Injected During Stabilization	Fines Production (gm/sq in)
Test 4	190-230	3	0.52
Test 5	110-150	3	0.47
Test 6	190-230	3	1.99
Test 7	190-230	3	2.08

Figure 5-15. Fines production for intermediate flow rate (second flow stage).

Figure 5-16 shows the production of fines concentration in the third flow stage (high flow rate). Although the initial peak showed by Test 4, which seems to be an outlier, Tests 6 and 7 present the higher amounts of fines production. The washout process is sustained for a shorter time for the third flow stage as the fine particles' production gets quickly mobilized due to the high flow rate. The fines production stabilization is achieved faster than for the previous two flow stages. This faster fines production stabilization happens, most likely, due to the excessive mobilization of fines during the first two flow stages.

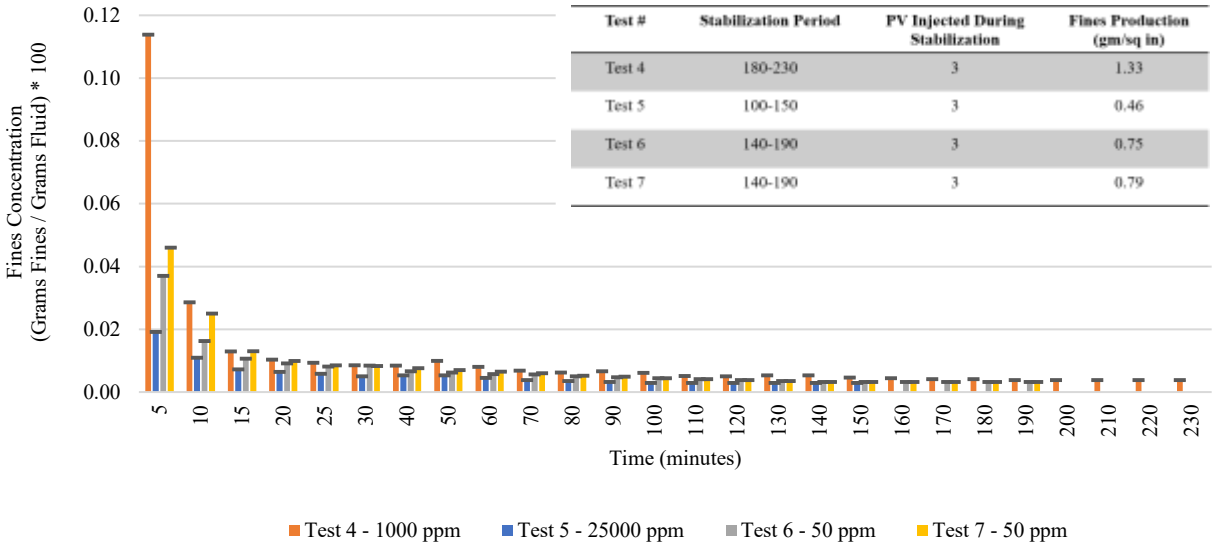

Test #	Stabilization Period	PV Injected During Stabilization	Fines Production (gm/sq in)
Test 4	180-230	3	1.33
Test 5	100-150	3	0.46
Test 6	140-190	3	0.75
Test 7	140-190	3	0.79

Figure 5-16. Fines production for high flow rate (third flow stage).

5.7. Gravel-Pack Impairment

Figure 5-17 displays the gravel-pack impairment correlation provided by Saucier (1974) and the gravel-pack impairment achieved by the end of the four tests performed. Tests 4 and 5 match Saucier's correlation as the gravel-pack impairment for Test 4 was 4%, while Test 5 showed a gravel-pack impairment of 6%. Saucier (1974) affirms that gravel-pack impairment is virtually non-existent for impairment of up to 10%. Therefore, Saucier (1974) gravel sizing criteria provided adequate gravel-pack impairment for salinity level in the range of 1,000 – 25,000 ppm NaCl (Tests 4 and 5). Tests 6 and 7, on the other hand, presented a considerably higher gravel-pack impairment, which was 30% and 34%, respectively.

The elevated gravel-pack impairment is justified by the 50-ppm low salinity level, representing the worst-case scenario for fines dispersion. As the salinity reaches a level of 50 ppm, the electrostatic forces, bonding the fines to the formation sand particles, are the lowest possible for clay material. Consequently, more fine particles are in dispersion within the carrier fluid. The high drag forces generated during the three flow stages contribute significantly to a high mobilization of fines, which leads Tests 6 and 7 to experience a high quantity of fine particles filling up the pore throats of gravel-pack structure. Therefore, the plugging effect of gravel-pack is more accentuated for a low salinity level of 50 ppm.

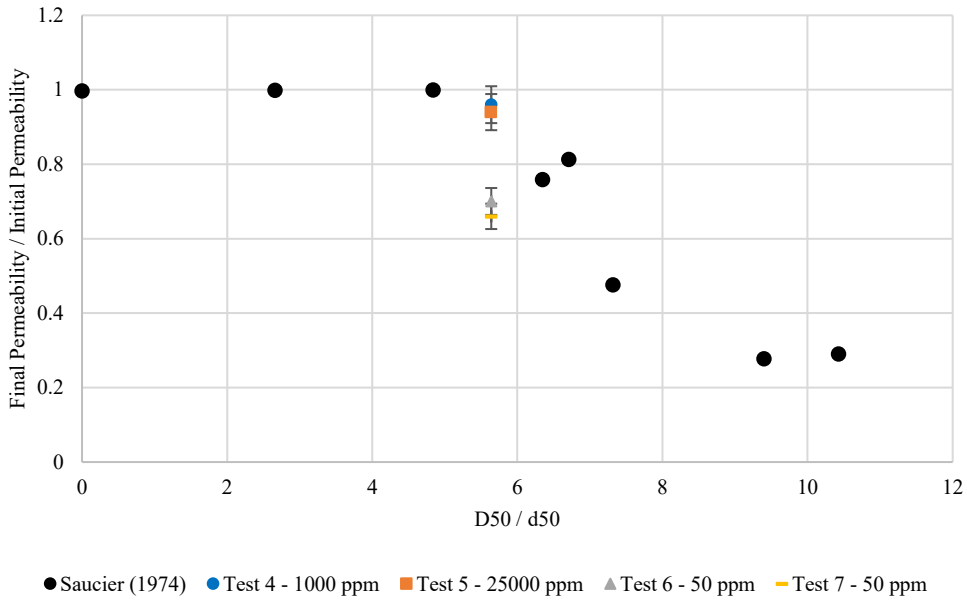

Figure 5-17. Gravel-pack impairment for the corresponding D50/d50 ratio.

In addition to the gravel-pack permeability alteration, the porosity variation was roughly estimated by applying the Konezy-Carman equation (Equation 5.1). This equation models the fluid flow in a packed bed of particles for laminar flow conditions (McCabe et al. 2005).

$$\frac{Ø^3}{(1-Ø)^2} = \frac{v*150}{ϕs^2*dp^2} * \frac{\mu*L}{\Delta P} \tag{5.1}$$

Where $Ø$ is the porosity of the packed bed, v is the superficial velocity, $ϕs$ is the sphericity of the particles in the packed bed, dp is the average diameter of grains composing the packed bed, μ is the viscosity of the fluid, L is the total height of the bed, and ΔP is the pressure drop across the total height. The initial gravel-pack porosity was 40%. The final porosity for Test 4 was 38.4%, while Test 5 registered a final porosity of 38.1%. Meanwhile, Tests 6 and 7 presented a final porosity of 36.5 and 36.25%, respectively. The tests with low salinity level, Tests 6 and 7, present lower final porosity values as more fines are expected to move inside the gravel-pack structure.

5.8. Particles Accumulation in the Gravel-Pack

The gravel-pack impairment can be further assessed by analyzing the amount and size of particles that filled up the gravel-pack structure by the end of each test. The gravel-pack was divided into two parts. The gravel top corresponds to the upper half of the gravel-pack structure, while the gravel bottom consists of the lower part of the gravel-pack. Both halves are 1-in long. Table 5-5

displays the number of particles, in weight percentage, retained by each sieve size (μm) during the sieving process of the samples extracted once each test was performed.

The upper part of the gravel presents a higher number of particles for all the tests. This higher number of particles is expected once the particles fill up the pore throats of the gravel-pack structure closest to the formation and gravel interface. The gravel-pack interface surrounding area has the highest expected damage caused by the accumulation of formation particles. This interface damage happens since as the formation particles start moving through the gravel-pack, they constrain some of the initially available gravel-pack pore throats. Therefore, the plugging effect on the upper part of the gravel structure should be higher, and fewer formation particles can reach the lower part of the gravel-pack.

Although most of the particles encountered in the gravel-pack structure are fines (smaller than 44 microns), some larger particles were also mobilized to the inside of the gravel-pack (see Table 5-5). However, Tests 6 and 7 differ from Tests 4 and 5 mainly by the larger number of fines placed inside the gravel-pack. The quantity of particles larger than 44 microns is roughly stable for all four tests. Therefore, although some formation particles could move inside the gravel-pack, the fines are the leading gravel-pack impairment agent. Some authors affirm that formation sand particles can enter the gravel-pack structure for a median grain size ratio equal to or larger than 6 (Saucier, 1974; Leone et al. 1990). However, there is an indication in the literature that even for a median grain size ratio of 5-6, formation particles can accumulate inside the gravel-pack (Tiffin et al. 1990). No formation particles, other than fines, were produced during anytime whatsoever.

Table 5-5. Amount and size of particles measured from gravel-pack core samples.

Test #	Sieve Size (μm)	wt. (%)	Test #	Sieve Size (μm)	wt. (%)
Test 4 Gravel Top	<44	1.43	Test 4 Gravel Bottom	<44	0.69
	44	0.68		44	0.32
	106	0.49		106	0.26
	150	0.47		150	0.17

Test 5 Gravel Top	<44	1.49	Test 5 Gravel Bottom	<44	0.68
	44	0.74		44	0.37
	106	0.46		106	0.29
	150	0.41		150	0.23
Test 6 Gravel Top	<44	2.69	Test 6 Gravel Bottom	<44	1.74
	44	0.83		44	0.39
	106	0.46		106	0.29
	150	0.39		150	0.21
Test 7 Gravel Top	<44	2.79	Test 7 Gravel Bottom	<44	1.79
	44	0.81		44	0.43
	106	0.48		106	0.30
	150	0.40		150	0.25

Tables 5-6, 5-7, 5-8, and 5-9 present the initial and final permeability measurements across the cell and the final fines content, in weight percentage, for each part of the cell. As the initial fines content for each test was 12%, all the cell parts lost fines by the end of the four tests. The measurement of fines across the cell is consistent and agrees with the permeability measurements. As more fines are mobilized from certain parts of the cell, higher is the corresponding part's permeability. The washing out process of fines from the formation and gravel interface is, apparently, efficient since the bottom's final permeability increases considerably for the four tests performed. Although Tests 6 and 7 present higher initial differential pressure for the bottom part of the cell (interface), the differential pressure declines over time, indicating that the gravel sizing can handle the passage of fines from the formation sand towards the gravel-pack structure. Tests 6 and 7 present final differential pressure for the interface lower than for Tests 4 and 5 (see Fig. 5-12). Therefore, the cell's bottom part final permeability is higher for Tests 6 and 7 than for Tests 4

and 5. This finding supports the statement that Saucier's (1974) gravel sizing design satisfactorily manages the fines accumulation at the formation and gravel interface.

Table 5-6. Permeability variation and final fines content across the cell for Test 4.

Cell Part	K Before Test (D)	K After Test (D)	Fines wt. (%)
Top	0.60	2.32	10.33
Middle	0.62	3.15	8.94
Bottom	0.60	3.00	9.33

Table 5-7. Permeability variation and final fines content across the cell for Test 5.

Cell Part	K Before Test (D)	K After Test (D)	Fines wt. (%)
Top	0.61	2.53	10.09
Middle	0.62	3.97	8.25
Bottom	0.60	2.92	9.38

Tables 5-8 and 5-9 display the permeability variation and the final fines content across the cell for Tests 6 and 7, respectively. There is a disagreement in the initial permeability values from Tests 6 and 7 compared to Tests 4 and 5. This permeability disagreement happens due to the initial high dispersion condition for the fines in the formation sand. As the salinity level for Tests 6 and 7 is 50 ppm, the fines are highly dispersed and most likely in suspension. Therefore, even though the flow rates used for permeability measurement are low (1.5-2.4 L/hr), fines are mobilized from the top and middle toward the bottom part of the cell during the permeability measurement. Consequently, an increase in initial permeability is registered for both top and middle parts of the cell, while the bottom part suffers a slight permeability decrease.

Table 5-8. Permeability variation and final fines content across the cell for Test 6.

Cell Part	K Before Test (D)	K After Test (D)	Fines wt. (%)
Top	0.78	2.56	10.03
Middle	0.73	3.50	8.74
Bottom	0.52	3.94	8.30

Table 5-9. Permeability variation and final fines content across the cell for Test 7.

Cell Part	K Before Test (D)	K After Test (D)	Fines wt. (%)
Top	0.80	2.83	9.73
Middle	0.72	3.53	8.69
Bottom	0.51	3.90	8.27

5.4. Conclusions

The assessment of Saucier's (1974) design criteria was performed on a highly non-uniform and high fines content PSD for OHGP investigation. The effect of salinity level was also encompassed in the test matrix proposed. A total of four tests were performed, as three different salinities were investigated (Test 4 – 1,000 ppm, Test 5 – 25,000 ppm, Test 6 – 50 ppm, Test 7 – 50 ppm). Test 7 is a repeatability test of Test 6, addressed to assessing the testing error.

The four tests followed the expectation regarding fines migration from the top toward the cell's bottom. Such a phenomenon is assessed by the differential pressure readings that confirm the top part's loss of fines. In contrast, the accumulation of fines occurs at the bottom part of the cell. However, some inconsistencies occurred as Test 5 (25,000 ppm NaCl) was expected to present the highest differential pressure in the cell's top part. This inconsistency is accounted to the packing procedure, a human source of error that demands a higher number of tests to be assessed and quantified.

The gravel-pack performance is evaluated considering the pressure buildup at the formation and gravel interface and the gravel-pack impairment. During the low flow rate injection, a similar pressure buildup is seen for the four tests, and the gravel-pack impairment is slightly higher for Tests 6 and 7 (50 ppm NaCl). The quantity of fines produced is similar during the first flow stage is similar in all the tests, despite the salinity level. Therefore, no distinction in the gravel-pack performance is available by the end of the first flow stage.

The intermediate flow rate injection shows higher pressure buildup at the formation and gravel-pack interface for Tests 6 and 7. As the drag forces generated for the second flow stage are higher than the first flow stage, the weaker electrostatic forces for Tests 6 and 7 allow higher fines mobilization toward the gravel-pack when compared to the first flow stage. Although the pressure buildup occurs at the initial phase of the second flow stage, the gravel-pack seems to handle the number of fine particles over time. The differential pressure at the interface for Tests 6 and 7 is slightly lower than the differential pressures for Tests 4 and 5 by the end of the second flow stage. On the other hand, the differential pressure in the gravel-pack is consistently higher for Tests 6 and 7 during the second flow stage completion. Even though the high drag forces can wash out some of the fines from the gravel-pack, the impairment caused by the high fines mobilization during low salinity tests (Test 6 and 7) persists to the flow stage completion.

The high flow rate injection presents similar trends than seen in the intermediate flow rate injection. However, some inconsistency is seen in the gravel-pack structure. Because the SRT facility provides a limited amount of fines in the system, few mobile fine particles are left by the end of the second flow stage, except for the cell's bottom part. Therefore, the high drag forces generated during the third flow stage end up washing out the gravel-pack structure. Consequently, the gravel-pack permeability is increased over the third flow stage. This output is the opposite of what is expected under field conditions since higher drag forces should lead to higher mobilization of fines towards the gravel-pack. The higher mobilization of fines would further impact gravel-pack permeability. Since there are not many fine particles migrating towards the bottom part of the cell, the gravel-pack allows the passage of fines. The gravel-pack impairment in Tests 6 and 7 are 30 and 34%, respectively. Meanwhile, gravel-pack impairment for Tests 4 and 5 is 4 and 6%, respectively.

Overall, Saucier (1974) sizing criteria seems to present satisfactory performance for salinity range of 1,000 - 25,000 ppm NaCl. However, once salinity reaches the worst-case scenario of 50 ppm, the gravel-pack permeability is severely impacted.

An assessment of the amount and size of particles encountered in the gravel-pack structure shows that most of these particles are smaller than 44 microns, therefore fines. However, following the literature, some particles larger than 44 microns were also carried and placed inside the gravel-pack. All the particles produced during the four tests were fines; therefore, no sand production was registered whatsoever.

Chapter 6 - Conclusions and Recommendations for Future Work

6.1. Main Results and Contribution

This research presented a modified Sand Retention Test (SRT) facility, which enabled the assessment of gravel sizing design for open-hole gravel-pack (OHGP) wells. The testing facility presented satisfactory repeatability, and it performed the replication of Saucier (1974) materials and operating parameters adequately. The results obtained boosted the confidence in the SRT design for OHGP investigation.

Although extensive work has been done on gravel sizing design, specific formations such as highly non-uniform and formations with high fines content had not been previously considered to assess gravel design criteria. Therefore, this investigation contributes to assessing Saucier's gravel sizing design criteria further. Furthermore, salinity level variation has not been accounted for in the literature available. Since salinity level plays an essential role in fines migration, it has been encompassed in this investigation.

The results obtained satisfactorily match the literature regarding the release of fine particles at variable salinity levels. As the salinity level increases, the number of fines mobilized decreases because of the higher electrostatic forces attaching the fines to the formation particles. Further fines mobilization results in higher pressure drops at the formation-gravel interface. However, over time, the interface differential pressure tends to decrease regardless of the salinity level. The gravel-pack impairment is severely affected by salinity levels of 50 ppm. However, the gravel-pack impairment is similar, and virtually non-existent, for the salinity level range of 1,000 – 25,000 ppm of NaCl.

The Saucier (1974) design criteria allowed the formation sand particles to enter the gravel-pack structure for the parameter ranges tested during this investigation. Although some formation particles larger than 44 microns entered the gravel-pack, the gravel-pack impairment is mainly caused by the fine particles. There was no production of particles larger than 44 microns whatsoever. The gravel sizing criteria proposed by Saucier (1974) works satisfactorily for the testing and operating conditions tested for the salinity range of 1,000 – 25,000 ppm of NaCl. For the salinity level of 50 ppm of NaCl, on the other hand, the sizing criteria do not perform adequately, as the gravel-pack impairment was excessive, jeopardizing the gravel-pack performance.

6.2. Recommendations for Future Work

The recommendations presented in this section aim to extend this investigation to understand further the limitations of the current gravel sizing criteria, Saucier (1974), widely used by the oil and gas industry. The recommendations can be considered individually or in combination.

6.2.1. Additional PSDs

Investigating additional highly non-uniform and high fines content PSDs can better understand if there is any limitation for the gravel performance when exposed to higher UC and higher fines content than previously tested. As the UC increases, the bridging phenomenon should be negatively affected, and therefore, more formation particles may enter the gravel-pack structure. Furthermore, higher fines content may lead to a higher accumulation of fines inside the gravel, impacting the final gravel-pack permeability.

6.2.2. Multiphase Production

As multiphase production is typical in gravel-pack scenarios and can lead to higher mobilization of fines, it should be considered for future investigations. Accounting for a multiphase flow could affect the gravel-pack performance as a higher quantity of fines entering the gravel-pack may generate a higher plugging effect.

6.2.3. Effect of pH

The pH also plays an essential role in fines migration, and pH may widely vary across different reservoirs and fields. Consequently, the possible range of pH levels for gravel-pack wells should be assessed and considered for the more in-depth investigation of gravel-pack sizing criteria' performance.

6.2.4. Effect of Clay Composition

The clays present different features depending on the clay mineralogy and structure. Therefore, clay features properties such as cation exchange capabilities, plastic behavior, and swelling behavior may vary, depending on the clay composition.

BIBLIOGRAPHY

Abram, M., and Cain, G. (2014). Particle-Size Analysis for the Pike 1 Project, McMurray Formation. Journal of Canadian Petroleum Technology. 53 (06): 339-354. SPE-173890-PA.

Aji, K. (2014). The Experimental and Theoretical Study of Fines Migration in Porous Media under Particle-rock Repulsion and Attraction. Doctoral dissertation, The University of Adelaide, Adelaide, Australia.

Barkman, H., and Davidson, H. (1972). Measuring Water Quality and Predicting Well Impairment. Journal of Petroleum Technology.

Bellarby, J. (2009). Well Completion Design (First ed., Vol. 56). Oxford, United Kingdom: Elsevier's Publications.

Bennion, D. B., Gupta, S., Gittins, S., & Hollies, D. (2009). Protocols for Slotted Liner Design for Optimum SAGD Operation. Petroleum Society of Canada.

Carlson, J., Gurley, D., King, G., Price-Smith, C., Water, F. (1992). Sand Control: Why and How? P41-53. Oilfield Review.

Coberly, C. J., & Wagner, E. M. (1937). Some Considerations in the Selection and Installation of Gravel Pack for Oil Wells. 20. Society of Petroleum Engineers.

Deruyck, B., Ehlig-Economides, C., Joseph, J. (1992). Testing Design and Analysis. Oilfield Review 4, no.2.

Derjaguin, B.V., Landau, L.D. (1941). Theory of the Stability of Strongly Charged Lyophobic Sols and of the Adhesion of Strongly Charged Particles in Solutions of Electrolytes. Acta Physicochim. URSS 14 (6), 633e662.

Elimelech, M., Gregory, J., Jia, X., Williams, R. (1995). Particle Deposition and Aggregartion: Measurement, Modelling, and Simulation. Butterworth-Heinemann, New-York, USA.

Gabriel, G. A., Inamdar, G. R. (1983). An Experimental Investigation of Fines Migration in Porous Media. Presented at the 58th Annual Technical Conference and Exhibition held in San Francisco, CA, October 5-8 1983.

Gregory, J., (1981). Approximate expressions for retarded van der Waals interactions. Journal of Colloid and Interface Science.

Guo, Y. (2018). Effect of Stress Build-up around SAGD Wellbores on the Slotted Liner Performance. Master of Science thesis, University of Alberta.

Haftani, M., Wang, C., Pallares, J. D. M., Mahmoudi, M., Fattahpour, V., Nouri, A. (2019). An investigation into the Effect of Brine Salinity on Fines Migration in SAGD Operations. SPE-195370-MS. Presented at the SPE Western Regional Meeting held in San Jose, California, USA, 23-26 April 2019.

Hill, K. E. (1941). Factors Affecting the Use of Gravel in Oil Wells. American Petroleum Institute.

Himes, R. E., Ruiz Jr., S. J. (1986). New Sidewall Core Analysis Techniques Improve Gravel Pack Design. SPE 14813. Presented at the Seventh SPE Symposium on Formation Damage Control of the Society of Petroleum Engineers held in Lafayette, LA, February, 26-27, 1986.

Ismail, I. M., Geddes, M. W. (2014). Fifteen Years of Expandable-Sand-Screen Performance and Reliability. SPE 166425. Presented at SPE Annual Technical Conderence and Exhibition, New Orleans, 30 Septem – 2 October 2013. SPE Drilling & Completion, June 2014.

Kia, F., Fogler, H. S., Reed, M. G., and Vaidya, R. N. (1987). Effect of Salt Composition on Clay Release in Berea Sandstones. SPE-16254-MS. Presented at the SPE International Symposium on Oilfield Chemistry, 4-6 February, San Antonio, Texas.

Khilar, K. Fogler, H. S. (1983). Water Sensitivity of Sandstones. Society of Petroleum Engineer Journal, 1983.

Khilar, K. C., and Fogler, H. S. (1984). The Existence of a Critical Salt Concentration for Particle Release. Journal of Colloid and Interface Science.

Khilar, K.C., Fogler, H.S. (1998). Migrations of Fines in Porous Media. Kluwer Academic Publishers, Dordrecht.

Ladd, R.S. 1978. Preparing Test Specimens Using Undercompaction. Geotechnical Testing Journal. 1(1): 16-23.

Latiff, A., 2011. A Thesis in Assessment and Evaluation of Sand Control Methods for a North Sea Field. Master's Thesis. Imperial College London, London, United Kingdom.

Layne, L., Gerwick, F. (1973). U.S. Patent No. 3,709,293. Washington, DC: U.S. Patent and Trademark Office. Issued January 9, 1973.

Leone, J.A., Mana, M. L., Parmley, J. B. (1990). Gravel-Sizing Criteria for Sand Control and Productivity Optimization. Presented at the 60th California Regional Meeting held in Ventura, California, April 4-6, 1990.

Mahmoudi, M. (2017). New Sand Control Design Criteria and Evaluation Testing for Steam Assisted Gravity Drainage (SAGD) Wellbores. Doctoral Thesis, University of Alberta.

Mahmud, H. B., Leong, V. H., Lestariono, Y. (2020). Sand production: A smart control framework for risk mitigation. KeAi Advancing Research Evolving Science.

Maly, G. P., Krueger, R. F. (1971). Improper Formation Sampling Leads to Improper Selection of Gravel Size. SPE 3041. Journal of Petroleum Technology JPT.

Matanovic, D., Cikes, M., & Moslavac, B. (2012). Chemical Consolidation. In Sand Control in Well Construction and Operation (pp. 85-94). Springer, Berlin, Heidelberg: Springer Environmental Science and Engineering.

Mishra, S., Ojha, K. (2015). Chemical Sand Consolidation: An Overview. Journal of Petroleum Engineering & Technology, *5*(2), 21-34. Retrieved from https://www.researchgate.net/publication/319743134_Chemical_Sand_Consolidation_An_Overview.

McCabe, W. L., Smith, J. C., Harriot, P. (2005). Unit Operations of Chemical Engineering (7th ed.), New York: McGraw-Hill.

Mohan, K.K., Fogler, H.S. (1997). Colloidally induced smectitic fines migration: existence of microquakes. American Institute of Chemical Engineers Journal. 43 (3), 565e576.

Nabawy, B., Geraud, Y. Rochette, P. (2009). Pore-Throat Characterization in Highly Porous and Permeable Sandstones. American Association of Petroleum Geologists Bulletin.

Oyeneyin, M. B., Peden, J. M., Hosseini, A., Ren, G., Bigno, T. (1992). Optimum Gravel Sizing for Effective Sand Control. Presented at the 67th Annual Technical Conference of the Society of Petroleum Engineers held in Washington, DC, October 4-7, 1992.

Penberthy, W.L.Jr. and Cope, B.J. (1980). Design and Productivity of Gravel-Packed Completions. SPE-8428-PA. Journal of Petroleum Technology.

Penberthy, W.L.Jr. and Shaughnessy, C.M. (1992). Sand Control. SPE Series. 109 pages.

Renpu, W. (2011). Advanced Well Completion Engineering, 3rd Edition. Elsevier. 736 pages.

Thodes, M. (1989). Introduction to Particle Technology. 1st Edition. Wiley. 474 pages.

Roostaei, M., Kotb O., Mahmoudi, M., Fattahpour, V., Wang C., Nouri, A., and Fermaniuk, B. (2018). An Experimental Investigation into Gravel Pack Performance in Steam-Drive Operations. SPE-190125-MS. Presented at the SPE Western Regional Meeting, 22-27 April, Garden Grove, California, USA 2018.

Ruckenstein, E., Prieve, D.C. (1976). Adsorption and Desorption of Particles and their Chromatographic Separation. American Institute of Chemical Engineers Journal.

Russell, T., Chequer, L., Borazjani, S., You, Z., Zeinijahromi, A. and Bedrikovetsky, P. (2018). Formation Damage during Improved Oil Recovery Fundamentals and Applications; Chapter 3: Formation Damage by Fines Migration: Mathematical and Laboratory Modeling, Field Cases.

Russell, T., Pham, D., Tavakkoli Neishaboor, M., Badalyan, A., Behr, A., Genolet, L., Kowollik, P., Zeinijahromi, A., and Bedrikovetsky, P. (2017). Effects of Kaolinite in Rocks on Fines Migration. Journal of Natural Gas Science and Engineering.

Santarelli, F., J., Ouadfel, H., Zundel, J. P. (1991). Optimizing the Completion Procedure to Minimize Sand Production Risk. SPE 22797, presented at the 66th SPE Annual Technical Conference and Exhibition, Dallas, Texas, USA, October 6-9, 1991.

Saucier, R. J. (1974). Considerations in Gravel Pack Design. Journal of Petroleum Technology, 26(02), 205-212.

Sarkar, A.K., Sharma, M.M. (1990). Fines migration in two-phase flow. Journal of Petroleum Technology 42 (05), 646-652.

Schwartz, D. H. (1970). Successful Sand Control Design for High Rate Oil or Water Wells. In SPE Reprint Series No 5, Well Completions. (pp. 184-195). Society of Petroleum Engineers of AIME.

Shahsavari, M. H., and Khamehchi, E. (2018). Optimum Selection of Sand Control Method Using a Combination of MCDM and DOE Techniques. Journal of Petroleum Science and Engineering.

Sokolov V. N., and Tchistiakov, A. A. (1999). Physico-Chemical Factors of Clay Particle Stability and Transport in Sandstone Porous Media. European Geothermal Conference Basel '99. September 28-30, 1999, Basel, Switzerland, Proceedings, Volume 2.

Stein, N. (1988). Determine Properties of Friable Formation Sands. World Oil 206, no. 3.

Syltoy, C. (2014). New Generation Expandle Sand Screens. Master Thesis Faculty of Scieence and Technology, University of Stavanger.

Tiffin, D., King, G., Larese, R., & Britt, L. (1998). New Criteria for Gravel and Screen Selection for Sand Control. SPE Formation Damage Control Conference. Lafayette: Society of Petroleum Engineers.

Tixier, M. P., Loveless, G. W., Anderson, R. A. (1975). Estimation of Formation Strength from the Mechanical Properties Log. Journal of Petroleum Technology 27th March 1975.

Tronvoll, J., & Fjaer, E. (1994). Experimental study of sand production from perforation cavities. International Journal of Rock Mechanics and Mining Sciences & Geomechanics Abstracts.

Van Oort, E., Van Velzen, G., and Leerlooijer, K. (1993). Impairment by Suspended Solids Invasion: Testing and Prediction. SPE-23822-PA.

Veeken C. A. M., Davies, D. R., Kenter C. J., Kooijman, A. P. (1991). Sand Production Prediction Review: Developing an Integrated Approach. SPE 22792. Presented at the 66th SPE Annual Technical Conference and Exhibition, Dallas, Texas, USA, October 6-9, 1991.

Xie, J. (2015). Slotted Liner Design Optimization for Sand Control in SAGD Wells. SPE-178457-MS. Presented at the SPE Thermal Well Integrity and Design Symposium held in Banff, Alberta, Canada, 23-25 November 2015.

You, Z., Badalyan, A., Yang, Y., Bedrikovetsky, P., Hand, M. (2019). Fines Migration in Geothermal Reservoirs: Laboratory and Mathematical Modelling. Volume 77. Pages 344-367.